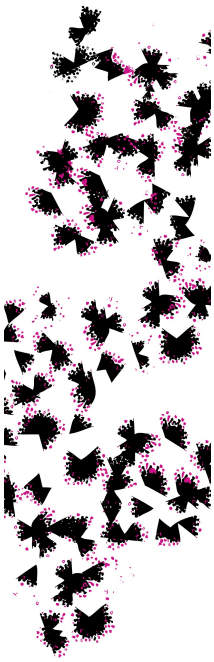

The characterization of an electrospun PVDF terpolymer for the design of a piezoelectric variable stiffness actuator

S.H.J. (Stephan) Visschers

BSc Report

Committee:
Dr. R. Carloni

August 2015

026RAM2015
Robotics and Mechatronics
EE-Math-CS
University of Twente
P.O. Box 217
7500 AE Enschede
The Netherlands

UNIVERSITY OF TWENTE.

MIRA CTIT
BIOMEDICAL TECHNOLOGY AND TECHNICAL MEDICINE

The characterisation of an electrospun PVDF terpolymer for the design of a piezoelectric variable stiffness actuator

Bachelor Assignment

S.H.J. Visschers

June 30, 2015

Abstract

Piezoelectric polymers are known for over 40 years now. polyvinyldifluoride and its copolymers have been applied to the field of electromechanical actuation, sensing, memory, and more. The terpolymer of vinyldifluoride, P(VDF-TrFE-CTFE), is a newly developed piezoelectric polymer material that is designed to be more electro active. To make use of this material in the design of a (variable stiffness) actuator, the mechanical and electrical properties of this material are characterised using specifically designed set-ups. The coupling between the two domains is investigated. The samples under investigation are unimorphs layered with support materials with thicknesses in the order of micrometres. Electric fields are applied to the samples by a modulated high-voltage source. Strain measurements are obtained using either visual data from a microscope or a laser reflection measurement. The force exerted by the samples is too small for conventional force measurement devices, so a specifically suitable contraption has to be designed to measure this force. Using these datasets, the electromechanical behaviour of the material can be characterised.

Contents

Abstract **1**

Table of Contents **3**

Introduction **4**
Theoretical Background . . . 4
Variable Stiffness Actuator . . . 4
Piezoelectricity . . . 4
Copolymer material . . . 5

1 Literature study **7**
1.1 Guo et al: longitudinal strain experiment . . . 7
1.1.1 Experiment . . . 7
1.1.2 Methods . . . 7
1.1.3 Results . . . 7
1.2 Cheng et al: transverse strain experiment . . . 8
1.2.1 Experiment . . . 8
1.2.2 Methods . . . 9
1.2.3 Results . . . 9
1.3 Cheng et al: characterisation of electrostrictive copolymers . . . 10
1.3.1 Experiment . . . 10
1.3.2 Methods . . . 10
1.3.3 Results . . . 11
1.4 Huang et al: copolymer and terpolymer based actuators . . . 14
1.4.1 Experiment . . . 14
1.4.2 Methods . . . 14
1.4.3 Results . . . 14
1.5 Conclusions . . . 16

2 Characterisation of P(VDF-TrFE-CTFE) **17**
2.1 Transverse strain experiment . . . 17
2.1.1 PC + RaMstix . . . 17
2.1.2 Amplifier . . . 17
2.1.3 High-Voltage source . . . 19
2.1.4 Fuse resistor and sample . . . 19
2.1.5 Voltage divider and ADC . . . 20
2.1.6 Leakage resistor . . . 20
2.1.7 Microscope and video recording . . . 20
2.1.8 LED signal . . . 20
2.1.9 Piezoelectric sample . . . 21

2.2 Experiment plan . . . 21
2.2.1 Strain measurement . . . 21
2.2.2 Resonance measurement . . . 24
2.2.3 Force measurement . . . 25
2.3 Results . . . 26
2.3.1 Strain measurement . . . 26
2.3.2 Resonance measurement . . . 28
2.3.3 Force measurement . . . 28

Conclusions and Discussion **30**

Bibliography **31**

Appendices **32**

A Data fit figures **33**

B Matlab point tracker script **36**

C Strain result plots **37**

Introduction

This Bachelor Assignment originates from the idea to have an alternative to the current design for a variable stiffness actuator, as the this current design needs two electric motors. If the mechanical properties of a material can be changed at will by applying an electrical potential, the need for the second motor might become obsolete. To this end, a specific piezoelectric polymer material will be characterised to determine its feasibility for the application in the construction of a electromechanical actuator.

Theoretical Background

Variable Stiffness Actuator

A Variable Stiffness Actuator (VSA) is a device that can realise a mechanical action, while continuously changing its mechanical stiffness. The mechanical stiffness is a measure for the amount of force that is needed to deform an object. Its reciprocal is the mechanical compliance. Compliance is in this context a desired property. If the compliance is constantly zero, the result would be an ordinary electronic DC motor.

A variable compliance is desired, to gain the ability to adapt the dynamic behaviour to an unknown environment. For example, in applications where machines (especially robots) work closely together with humans. This reduces the risks of injuries, as the robot will be able to reduce the impact in the event of a collision.[5]

Piezoelectricity

Piezoelectricity is the phenomenon that an electric field is established across a material specimen, because of an induced polarization, by the application of external forces.[8] The piezoelectric effect is a reversible process. This means that a material that exhibits the piezoelectric effect will also exhibit the converse piezoelectric effect. This converse effect entails that a mechanical strain will be induced when an electric field is applied across the specimen. This converse effect will be used for the research conducted in this thesis.

Piezoelectricity couples mechanical and electrostatic energy. This coupling can be described with the independent variables:

D Displacement field
E Electric field
ε Mechanical strain
σ Mechanical stress

The piezoelectric coefficient is then defined as:

$$d = \left(\frac{\partial D}{\partial \sigma}\right)_E = \left(\frac{\partial \varepsilon}{\partial E}\right)_\sigma \tag{1}$$

From equation 1 it is apparent that the piezoelectric coefficient is a measure for the induced strain by an applied electric field under constant stress conditions.

The elastic energy of a piezoelectric body, which is deformed under isothermal conditions, can be described by the Gibbs free energy potential:

$$G = U - TS = -\frac{1}{2}\kappa^{\sigma}E^2 - \frac{1}{2}s^E\sigma^2 - d \cdot E\sigma \tag{2}$$

where κ^{σ} is the permittivity at constant stress and s^E is the elastic compliance at constant electric field.[10] By means of partial differentiation, the equations of state are obtained:

$$\begin{aligned} \varepsilon &= -\left(\frac{\partial G}{\partial \sigma}\right)_E = s^E\sigma + d \cdot E \\ D &= -\left(\frac{\partial G}{\partial E}\right)_{\sigma} = \kappa^{\sigma}E + d \cdot \sigma \end{aligned} \tag{3}$$

Because these equations are coupled, they can be combined in matrix form:

$$\begin{pmatrix} \varepsilon \\ D \end{pmatrix} = \begin{bmatrix} s^E & d \\ d & \kappa^{\sigma} \end{bmatrix} \begin{pmatrix} \sigma \\ E \end{pmatrix} \tag{4}$$

The coupling coefficient of this matrix is:

$$k^2 = \frac{d^2}{s^E\kappa^{\sigma}} \tag{5}$$

This coupling coefficient can be used to relate the material constants for different conditions to each other:

$$\begin{aligned} s^D &= s^E\left(1 - k^2\right) \\ \kappa^{\varepsilon} &= \kappa^{\sigma}\left(1 - k^2\right) \end{aligned} \tag{6}$$

These relations can be used to describe the piezoelectric effect.

The origin of the piezoelectric effect is in the asymmetric distributions of charges inside the particles of the material. In the case of ceramic materials, those charges are the ions inside the crystalline structure of the molecules. In the case of polymers, like PVDF, the charges are the atoms inside the functional groups of the molecules that are folded in a certain orientation.

Copolymer material

P(VDF-TrFE) is short for the copolymer of vinylidene fluoride and trifluoroethylene. Its structural formula is displayed in figure 1. The PVDF polymer and its copolymer can crystallize in five different phases (α to ε). The α phase is non-polar, which means the internal dipoles of the material are randomly orientated. The β phase is the most polar and thus the desired property for the material. To ensure the correct polarization of the polymer, different production techniques can be used.

Terpolymer material

P(VDF-TrFE-CTFE) is short for the terpolymer of vinylidene fluoride, trifluorotethylene and chlorotrifluoroethylene. Its structural formula is displayed in figure 2. The addition of the third monomer in the chain increases the entropy in the material and accordingly, decreases the elastic modulus. The applied production technique for the material used in this experiment is electrospinning.

Electrospinning

An intense electric field of more than 107 volts per metre is applied to a cone containing the polymeric solution. The polymer is extruded through a nozzle and deposited on a grounded substrate. The substrate is continuously in motion. Through intense mechanical stretching and electrical poling during the process, the dipoles are aligned and the need for additional poling is minimized.[1]

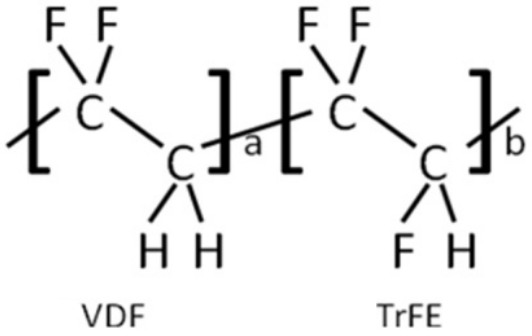

Figure 1: The structural formula of P(VDF-TrFE)

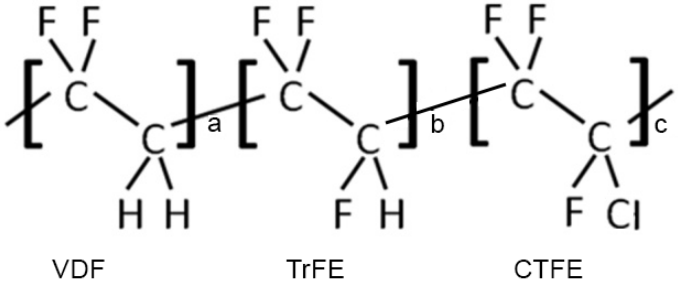

Figure 2: The structural formula of P(VDF-TrFE-CTFE)

1. Literature study

1.1 Guo et al: longitudinal strain experiment

1.1.1 Experiment

In this experiment, Guo et al[6] use a specially designed dilatometer to measure the longitudinal strain (parallel to the electric field applied) of piezoelectric samples.

1.1.2 Methods

The set-up consists of different stages (visible in figure 1.1):

- Sample platform
- Sensor element
- Protect circuit
- Low-noise amplifier
- Lock-in amplifier
- Function generator
- High-voltage amplifier
- Oscilloscope

Two sample platforms were designed for different experimental conditions. For relatively low applied electric fields, the sample is deposited onto a glass substrate with a thin electrode layer in between. With two metal pins the positive and negative contacts are made upon the electrodes. This substrate is placed in a Teflon container. For high electric fields, a brass container with in the middle a hemisphere edged out upon which the sample rests can be used. With this platform, the sample can be immersed in an insulating oil to avoid sparks. The hemisphere provides the positive contact and the ground terminal is a metal pin pushed against the edge of the sample.

The sensor element consists out of a stainless steel pin attached to a piezoelectric bimorph. When the pin is moved up and down by the sample, the bimorph will bend and accordingly, an electric current will be generated by the bimorph.

To protect the measurement devices from a sudden voltage pulse when the sample breaks, a protection circuit is included that will short-circuit if the input exceeds 0.6 volts.

The low-noise amplifier is a current pre-amplifier that reduces the interference effect of the cables on the signal and converts the signal to a measurable voltage output.

The lock-in amplifier is used to measure very small signals in a noisy background.

The electric field applied to the sample was generated by an arbitrary function generator in combination with the high-voltage amplifier (which can generate a signal in the range of 600 kilovolts).

The oscilloscope is used to check the input signal.

1.1.3 Results

Since the experiment was about designing an accurate strain measurement set-up, most of the results are about the reliability and accuracy of the set-up. Among the results was also the electric field - strain relationship of

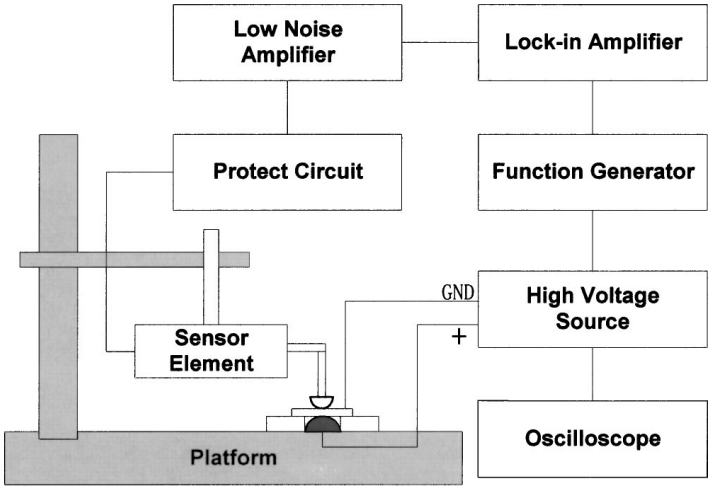

Figure 1.1: The experimental set-up of Guo et al

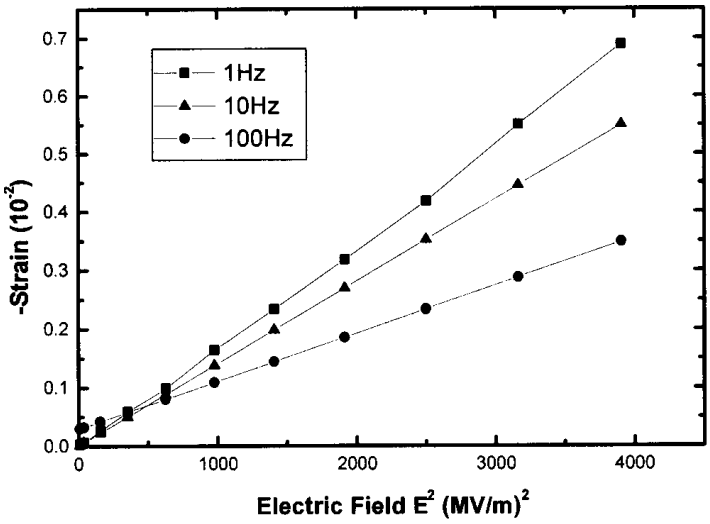

Figure 1.2: Strain results of Guo et al

a proton irradiated P(VDF-TrFE) sample with 70 to 30% mole fraction, which is displayed in figure 1.2. Since the relation is expected to be quadratic, the x-axis displays the square of the applied electric field. Then the resulting graph becomes linear, which supports the expectation of a quadratic relationship. The results show also that for increasing frequency, the strain decreases.

1.2 Cheng et al: transverse strain experiment

1.2.1 Experiment

In this experiment, Cheng et al[2] design a set-up specifically for accurate measurement of the transverse strain (perpendicular to the electric field) of soft polymer films. The performance is tested using electron irradiated P(VDF-TrFE) polymer films with a molar ratio of 65/35. The motivation for this experiment was to make an accurate, non-contact measurement device to detect the strain response without imposing an increasing load. The cantilever that holds the sample does impose a load, but this load is a constant value that can be varied over a wide range.

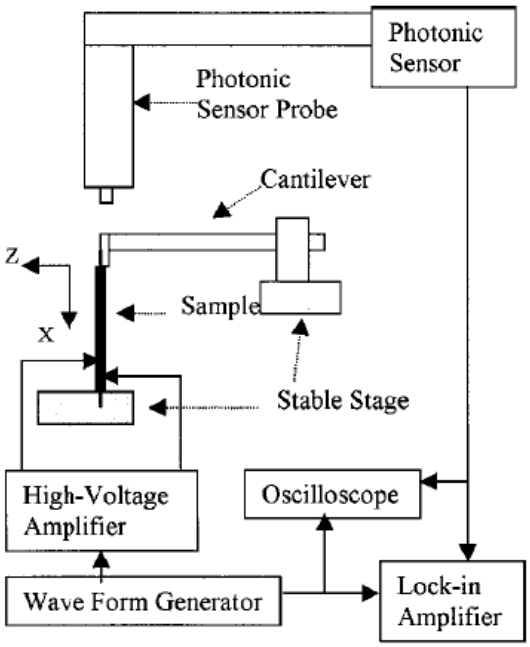

Figure 1.3: The transverse strain experiment performed by Cheng et al

1.2.2 Methods

The set-up consists of different stages (visible in figure 1.3):

- Sample platform
- Cantilever stage
- Photonic sensor + probe
- Lock-in amplifier
- Function generator
- High-voltage amplifier
- Oscilloscope

The photonic sensor probe measures the distance to the tip of the cantilever, which is directly attached to the polymer sample. To ensure that the transverse strain response is correctly measured, the sample has to remain in a vertically aligned orientation. To be able to correct the orientation, the sample platform is able to translate along the x-y-z axes and rotate about the x-axis.

The free end of the sample is connected to the free end of the cantilever, which will induce a static load upon the sample, due to gravity acting on the cantilever. The cantilever enables the optic probe to measure the strain of the sample. The static load can be varied by changing the dimensions of the cantilever, which enables the study of electromechanical behaviour under different loading conditions.

The output of the photonic sensor is measured through a lock-in amplifier for small strains, and the oscilloscope for larger strains. The lock-in amplifier makes it possible to measure a signal of a few microvolts in a 10 millivolts noise background.

The function generator in combination with the high voltage amplifier applies the electric field signal to the sample.

1.2.3 Results

The relevant results obtained by the experiment of Cheng et al are displayed in figure 1.4. The first figure shows the transverse strain response to an increasing electric field for samples that were activated under different

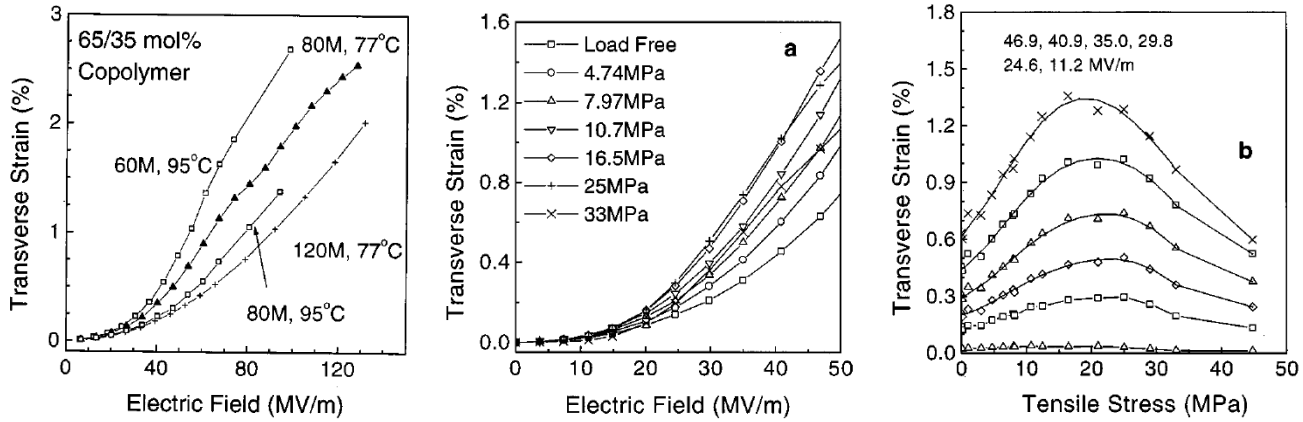

(a) Transverse strain response vs electric field under different electron irradiation conditions

(b) Transverse strain response vs electric field under different mechanical load conditions

(c) Transverse strain response vs mechanical load under different electric field conditions

Figure 1.4: Transverse strain results of Cheng et al

electron irradiation conditions. In the second figure, the transverse strain response to an increasing electric field under different mechanical loads for the most active sample is shown. In the third figure, the transverse strain response for an increasing load is plotted for various electric field strength. You can see that the strain first increases, and then, after reaching a maximum, will decrease.

Discussion

The result visible in figure 1.4b shows a quadratic relationship between the strain response and the applied electric field. This behaviour was predicted by Cheng et al with the electrostrictive model described by equation 1.1. In this equation, the $d_{31}E$ is the piezoelectric contribution and the $M_{31}E^2$ is the electrostrictive contribution.

$$S(E) = d_{31}E + M_{31}E^2 \tag{1.1}$$

The results visible in 1.4c show a change in behaviour, that Cheng et al contribute to a phase change as a result of the increasing load.

1.3 Cheng et al: characterisation of electrostrictive copolymers

1.3.1 Experiment

This experiment[3] uses previously devised set-ups to characterise the electromechanical properties of P(VDF-TrFE) copolymers. The transverse strain set-up described before were also utilized in this research paper.

1.3.2 Methods

The experiment consisted out of several set-ups:

- The longitudinal strain set-up of Su et al[11] on which the set-up of Guo et al is based.
- The transverse strain set-up of Cheng et al.
- A ”TA Instrument model 2980” dynamic mechanical analyzer to determine the elastic modulus of the polymer films.
- An HP 4194A impedance analyzer was used to characterize the resonance behaviour of the films under dc electric bias field.

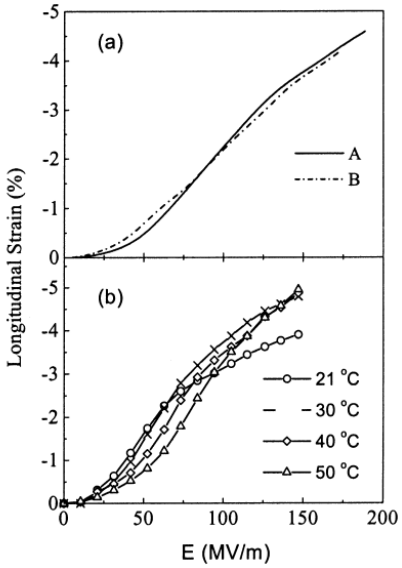

Figure 1.5: Longitudinal strain results of Cheng et al under varying conditions

The samples the article focuses on are P(VDF-TrFE) films with a molar fraction of 65/35 and 68/32 prepared under varying temperatures and irradiation conditions.

1.3.3 Results

The longitudinal strain results, measured at room temperature, of the 65/35 sample is given in figure 1.5a for a stretched and unstretched fabrication step. In figure 1.5b, the longitudinal strain results of the 68/32 sample are shown for varying temperatures during measurements.

The transverse strain results for the stretched samples as a function of the amplitude of the electric field oscillating with 1 Hz are displayed in figure 1.6. Figure 1.6a shows the transverse strain response for different samples. Sample A is the 68/32 sample and the B, C and D are the 65/35 samples with different irradiation conditions. Figure 1.6b shows the transverse strain results for the 68/32 copolymer film measured at different temperatures.

The electrical impedance of the stretched 68/32 copolymer film is plotted as a function of the frequency of the applied field in figure 1.7. This frequency dependence is shown in the figure for an increasing DC bias of the electric field. The graphs show a capacitive behaviour, but also subtle peaks disturbing the $Z_C = \frac{1}{2 \cdot \pi \cdot f}$ relationship. These subtle peaks are the locations of the resonance and antiresonance frequencies. The resonance frequency is related to the mechanical properties of the material. Equation 1.2 shows the relationship between the Young's Modulus and the resonance frequency, where s_{11}^E is the elastic compliance along the stretching direction, ρ is the mass density of the material, ℓ is the length of the film and f_s is the resonance frequency. Equation 1.3 shows the relation between the electromechanical coupling factor in stretching direction and the resonance frequencies, where k_{31} is the electromechanical coupling factor and f_p is the antiresonance frequency. From these relations, the data plotted in figure 1.8 is derived.

$$Y = \frac{1}{s_{11}^E} = 4\rho f_s \ell \tag{1.2}$$

$$\frac{k_{31}^2}{1 - k_{31}^2} = \frac{\pi}{2} \frac{f_p}{f_s} \tan\left(\frac{\pi}{2} \frac{f_p - f_s}{f_s}\right) \tag{1.3}$$

Another relevant experiment that Cheng et al performed in this article was a series of measurements of the field induced strain under mechanical loads. The results of this measurement are displayed in figure 1.9.

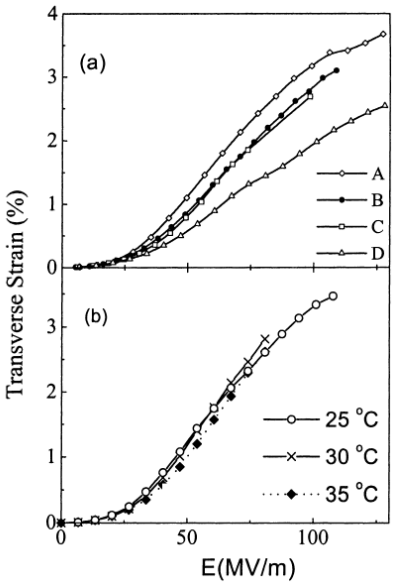

Figure 1.6: Transverse strain results along the stretching direction of Cheng et al under varying conditions

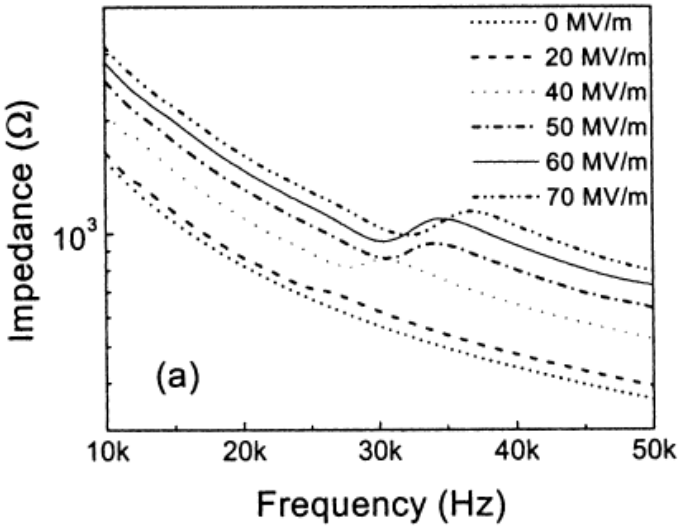

Figure 1.7: Frequency dependence of the impedance for an increasing DC bias field

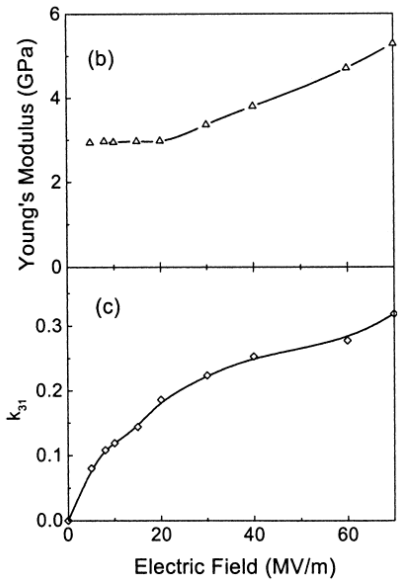

Figure 1.8: Mechanical properties as a function of the electric field strength

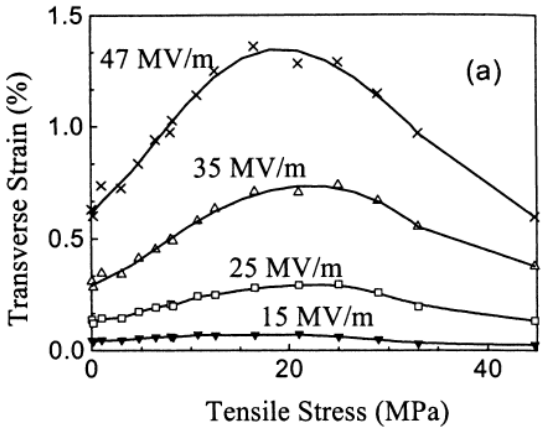

Figure 1.9: Mechanical load dependence of the transverse strain for an increasing field strength

It shows the transverse strain dependence on an increasing mechanical load (tensile stress) for an increase in electric field strength.

Furthermore, to analyse the mechanical motion of a unimorph electroactive polymer actuator, equations 1.4 and 1.5 are introduced.

$$\delta = \frac{3L^2}{2t} \frac{2AB(1+B)^2}{A^2B^4 + 2AB(2+3B+2B^2)+1} S_1 \tag{1.4}$$

$$F = \frac{2wt^2Y}{8L} \frac{2AB}{(AB+1)(1+B)} S_1 \tag{1.5}$$

In these equations the symbols represent the following parameters:

$\delta =$ tip displacement of the unimorph
$F =$ blocking force of the actuator
$L =$ length of the unimorph

$w =$ width of the unimorph
$t =$ thickness of the unimorph
$S_1 =$ transverse strain
$Y =$ Young's modulus along the length direction
$A =$ ratio of Young's modulus and to thickness of the active film
$B =$ ratio of the thickness of the substrate and the thickness of the active film

1.4 Huang et al: copolymer and terpolymer based actuators

1.4.1 Experiment

Huang et al[7] uses the experimental set-ups developed by Cheng et al to characterise two modified P(VDF-TrFE) copolymer materials. The first modification is high energy electron irradiation. The second modification is the introduction of a third monomer into the chain, namely chlorofluoroethylene (CFE). Both modifications aim to introduce defects in the lattice structure, with the expectation that the field induced strain increases.

1.4.2 Methods

The experiment consisted out of several set-ups:

- The longitudinal strain set-up of Su et al[11] on which the set-up of Guo et al is based.
- The transverse strain set-up of Cheng et al.
- A "TA Instrument model 2980" dynamic mechanical analyzer to determine the elastic modulus of the polymer films.

The samples consist out of stretched irradiated 68/32 P(VDF-TrFE) copolymer film, unstretched 62/38/4 P(VDF-TrFE-CFE) terpolymer film, unstretched 68/32/9 P(VDF-TrFE-CFE) terpolymer film and stretched 68/32/9 P(VDF-TrFE-CFE) terpolymer film. The stretching of the polymer films was done uniaxially up to 5 times the original length along the transverse strain direction. This stretching is expected to increase the transverse strain along the stretching direction. The applied electric fields had a frequency of 1 Hz. All measurements were taken at room temperature, unless specifically indicated otherwise.

1.4.3 Results

Figure 1.10a shows the longitudinal strain response of the irradiated copolymer as a function of the applied field strength. Figure 1.10b shows the transverse strain response of the irradiated copolymer as a function of the electric field strength. Figure 1.10c shows the deduced electromechanical coupling factor of the copolymer sample as a function of the increasing electric field strength.

Figure 1.11 shows the longitudinal strain response of the 62/38/4 terpolymer as a function of the electric field strength.

Figure 1.12 shows the longitudinal strain response, the transverse strain response for the unstretched sample and the transverse strain response for the stretched sample of the 68/32/9 terpolymer of Huang et al, respectively.

In addition, Huang et al provided an overview of the mechanical properties in the longitudinal direction of different electroactive polymers, which is shown in table 1.1, where S_M is the maximum strain and Y is the Young's modulus.

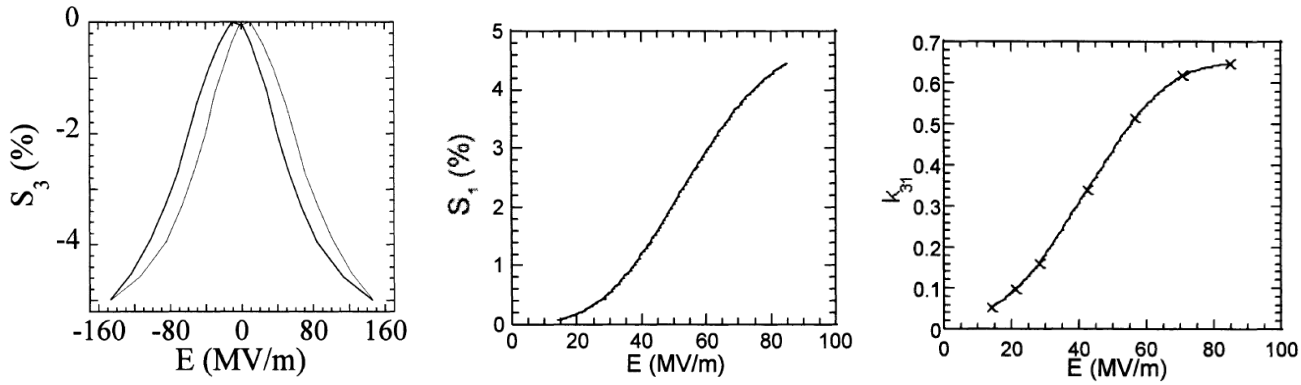

(a) Longitudinal strain response (b) Transverse strain response (c) Coupling factor variation

Figure 1.10: Results for the copolymer sample of Huang et al

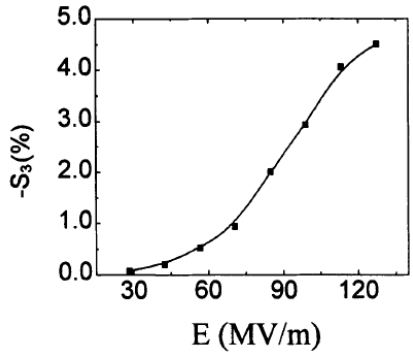

Figure 1.11: Longitudinal strain response of the 62/38/4 terpolymer vs. electric field strength

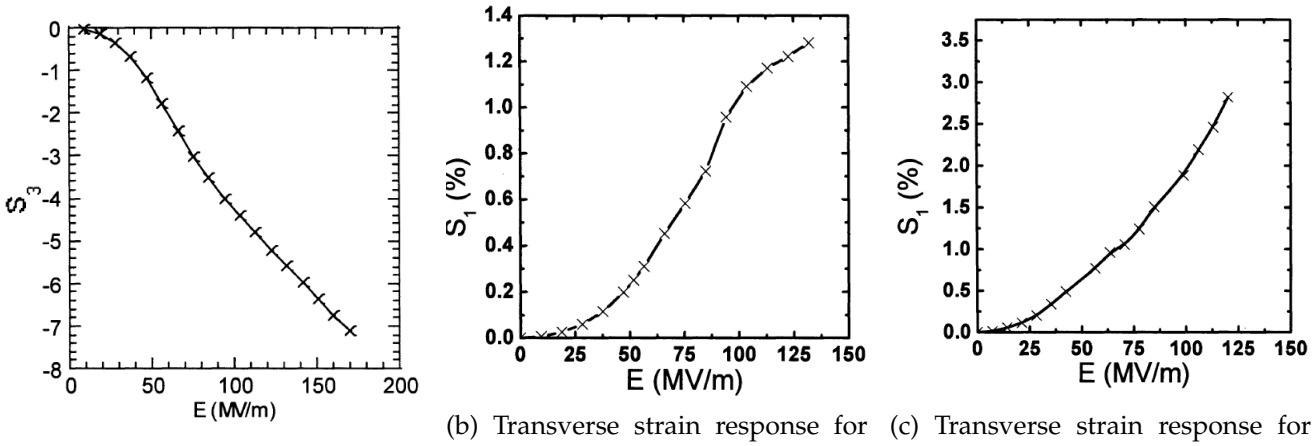

(a) Longitudinal strain response (b) Transverse strain response for the unstretched sample (c) Transverse strain response for the stretched sample

Figure 1.12: Results for the 68/32/9 terpolymer sample of Huang et al

Polymer Material	S_M (%)	Y (GPa)
Piezoelectric P(VDF-TrFE)	0.2	3.3
High-energy electron irradiated P(VDF-TrFE)	-5	0.4
P(VDF-TrFE-CTFE)	-4	0.4
P(VDF-TrFE-CFE) 62/38/4	-4.5	1.2
P(VDF-TrFE-CFE) 68/32/9	-7	0.3

Table 1.1: Mechanical properties overview of electroactive polymers

1.5 Conclusions

From table 1.1 a conclusion can be made that there is at least an inverse correlation between the Young's Modulus of the material and the maximum strain. This correlation can be explained by the fact that both properties are related to the crystal lattice structure. When the elastic modulus increases, the amount of force needed to compress the material increases as well. Therefore, the maximum strain for the same electric field decreases.

By looking at the transverse strain behaviour of the materials studied in the previously mentioned articles, the strain expected in the experiment conducted in this document is expected to be similar to the transverse strain of the stretched terpolymer sample of Huang et al. Thus, as a guideline, a strain of 2% for an electric field of 100 MV/m. However, since the samples used are fabricated using unconventional methods, it is uncertain how accurate the comparison with these results will be.

2. Characterisation of P(VDF-TrFE-CTFE)

2.1 Transverse strain experiment

In order to obtain a series of measurements of the transverse strain of the samples, an experimental set-up is build as displayed in figure 2.1. The individual parts of the experimental set-up will be elaborated on in detail. The transfer functions are used to calculate the theoretical signal that will be applied before it is applied to the sample.

2.1.1 PC + RaMstix

To modulate and control the electric field applied to the samples, an FPGA-board (the RaMstix) made by the research group is connected to a PC with the 20-sim and 20-sim 4C software package. In this composition, a signal is created in a 20-sim sub-model. The sub-model is converted to C-code and compiled using 20-sim 4C, and send to the FPGA on the board. The resulting signal is applied to a Digital-to-Analog converter installed on the board. This converts the digital signal to an analog signal ranging from -1 to +1 volts (according to the template that is included in the driver software of the RaMstix). For the modulation of the electric field, we need only a positive voltage. Therefore, the signal is between 0 and +1 volts.

The connector with the next stage has 3 pins. A positive terminal, a negative terminal and a ground reference. In the composition that is used in this experiment, the negative terminal is connected to the ground, because we only need the positive output. This has as an effect that the resulting output of the DAC is actually approximately half of the digitally specified voltage. To be more exact, the transfer of this input was measured, using the Fluke 175 multimeter, for several values and fitted to a first order polynomial relation using Matlab. The fitting curve is visible in figure A.1. The determined relation with an R^2 value of 1 (which is a measure for the accuracy of the fit), is:

$$V_{out} = 0.5037 \cdot V_{in} + 0.01306 \tag{2.1}$$

2.1.2 Amplifier

The analog output signal of the DAC is fed into an amplifier to obtain a voltage ranging from 0 to +10 volts. The amplifier is an active, non-inverting operational amplifier circuit including a filter. The amplifier enhances

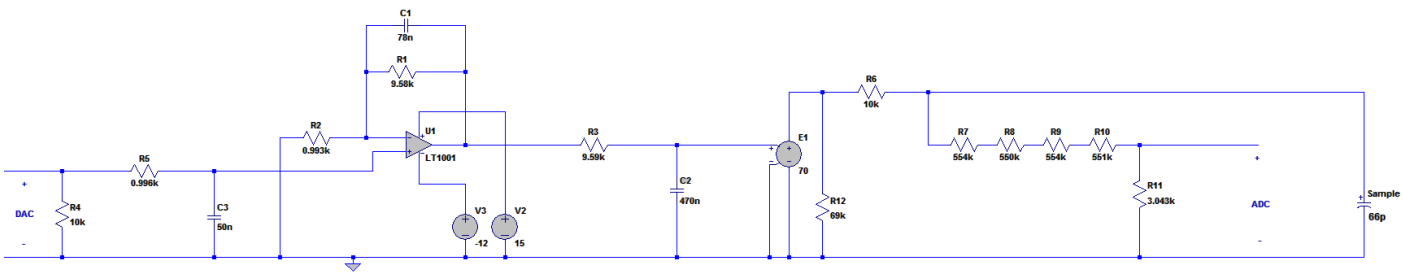

Figure 2.1: Complete set-up schematic

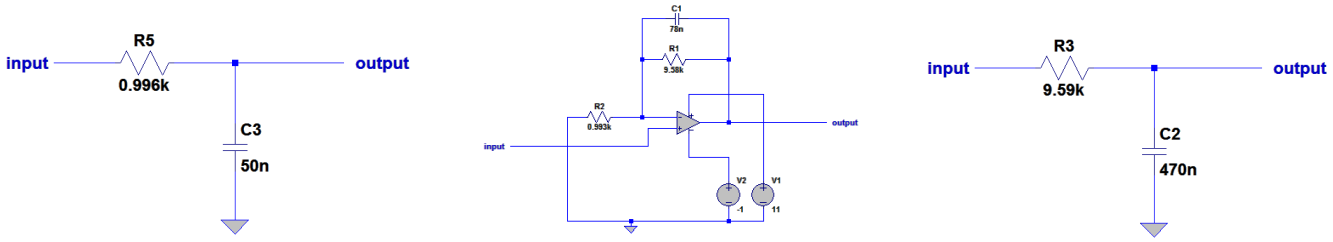

(a) Passive low pass filter before amplification

(b) Non-inverting amplifier with low pass filter

(c) Passive low pass filter after amplification

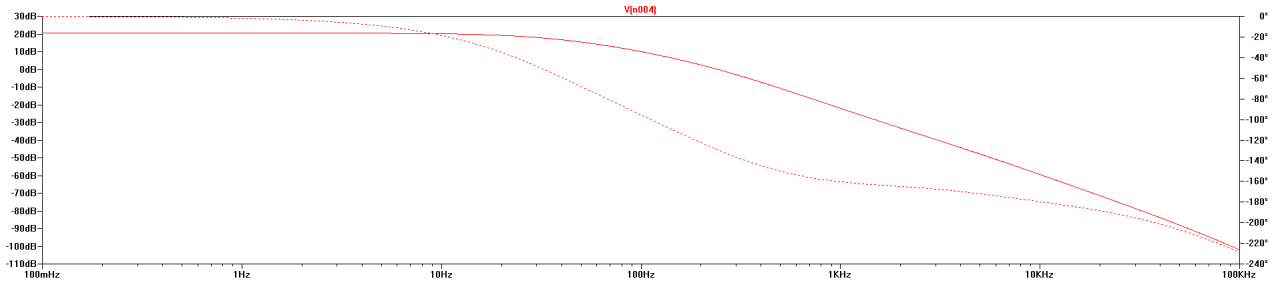

Figure 2.3: The frequency response of the amplifier stage

the noise in the system as well. To reduce the noise, a low-pass filter is included before, during and after the amplification, each with a different cutoff frequency. The specific values are chosen based on availability of the components. The passive low pass before the amplification is visible in figure 2.2a. Its cutoff frequency is determined by:

$$f_c = \frac{1}{2\pi R_5 C_3} = 3195.9\ Hz \tag{2.2}$$

The filter during the amplification stage is a capacitor added in parallel to the feedback resistor. This amplification stage is depicted in figure 2.2b. This will achieve a low pass filter with a cutoff frequency of:

$$f_c = \frac{1}{2\pi C_1 R_1} = 213\ Hz \tag{2.3}$$

The desired amplification of the operational amplifier circuit is achieved by tuning the ratio of the two resistors R_1 and R_2. The theoretical amplification factor of this stage is:

$$\frac{V_{out}}{V_{in}} = 1 + \frac{R_1}{R_2} = 1 + \frac{9580}{993} = 10.648 \tag{2.4}$$

The passive filter after the amplification stage is displayed in figure 2.2c. Its cutoff frequency is determined by:

$$f_c = \frac{1}{2\pi R_3 C_2} = 35.3\ Hz \tag{2.5}$$

The transfer of this amplification stage was measured for an applied DC voltage and fitted to a first order polynomial relation, visible in figure A.2. The determined relation, with an R^2 value of 1, is:

$$V_{out} = 10.11 \cdot V_{in} + 0.01962 \tag{2.6}$$

The frequency response of the entire amplifier stage is shown in a bode plot in figure 2.3. The operating range of this stage exceeds the limit of the next stage, so it is not limited by the amplifier electronics.

2.1.3 High-Voltage source

The high-voltage source used is a Technix SR 300 Watts. This HV-source has a manual safety lock, two potentiometers to regulate the output voltage and maximum current, and a remote connection to modulate these settings externally. This remote connection uses a D-sub DA-15 connector as an input. The pin configuration of this connector are as follows:

1. By shorting this pin to the logic ground, remote control is allowed
2. Inhibit Control (not used)
3. Current Monitor (not used)
4. Voltage Monitor (not used)
5. By shorting this pin to the logic ground, the high voltage output is unlocked
6. Interlock Monitor (not used)
7. Fault Monitor (not used)
8. By shorting this pin to the logic ground, the digital high voltage lock is lifted
9. Analog Ground Reference
10. HV On Monitor (not used)
11. End of Charge Monitor / Regulation Mode Monitor (not used)
12. Voltage Setting: 0 to 10 V (with reference to analog ground) = 0 to 100% of maximum output voltage (= 700 V)
13. Logic Ground Reference
14. +10V Reference (not used)
15. Current setting: 0 to 10 V (with reference to analog ground) = 0 to 100% of maximum output current (= 429 mA)

Thus by providing a 0 to +10 volts signal to pins 12 and 15, the high voltage source is modulated by the RaMstix. An important phenomenon to keep in mind with this set-up is the slew rate of the HV-source. As it needs time to charge to a certain voltage level, the behaviour in time is strongly dependent on the slew rate i.e. the maximum time derivative of the output voltage. The slew rate can be related to the settling time, which is the time needed to approach a certain step in the output within a certain error margin. The settling time is defined in the documentation of the HV-source to be around 100 milliseconds for voltages below 100 kilovolts.[12]

The transfer from the remote input voltage to the voltage applied to the sample was measured and subsequently fitted to a 6th order polynomial relation to increase accuracy. This 6th order polynomial fit is displayed in figure A.3. The determined relation with an R^2 value of 1, is:

$$V_{out} = -1.163E-5 \cdot V_{in}^6 + 0.0001715 \cdot V_{in}^5 - 0.0008607 \cdot V_{in}^4 + 0.002283 \cdot V_{in}^3 - 0.004252 \cdot V_{in}^2 + 69.82 \cdot V_{in} + 0.2795 \tag{2.7}$$

2.1.4 Fuse resistor and sample

Safety is always an important issue. High voltages are used in the experiments that are described in this paper. Therefore, appropriate safety measures must be taken. One of those safety measures is to ensure that the circuit where the high voltages are applied are enclosed in a box during experiments, so that no one can touch the circuit when it is dangerous. Another safety measure is the fuse resistor that is added to the circuit (R_6). This resistor should act as a fuse when a connection is short-circuited. The power dissipated will then be so high that the resistor will burn through and break the connection.

The sample was tested by a Hameg HM8118 LCR-bridge. A capacitance of 66 pF was observed. The resistance was in the order of 500 mega ohms, but this value changed with frequency, which is expected due to the capacitive behaviour.

2.1.5 Voltage divider and ADC

To ensure that the voltage applied to the sample is known, a voltage divider is constructed parallel to the sample. This enables the Analog-to-Digital converter of the RaMstix to measure the applied signal. The ADC has an operating range of -2.5 to +2.5 volts according to the template. The theoretical division factor of the divider is:

$$\frac{V_{out}}{V_{in}} = \frac{R_1 1}{R_7 + R_8 + R_9 + R_1 0 + R_1 1} = \frac{3.043}{554 + 550 + 554 + 551 + 3.043} \approx 1.376 \cdot 10^{-3} \tag{2.8}$$

Since V_{out} is the value measured by the ADC, we need the inverse of this relation to find the actual voltage applied to the sample. The inverse of equation 2.8 is:

$$\frac{V_{in}}{V_{out}} = \left(1.376 \cdot 10^{-3}\right)^{-1} = 726.93 \tag{2.9}$$

Again, the actual transfer was measured and fitted to a 6th-order polynomial relation, displayed in figure A.4. The determined relation with an R^2 value of 1, is:

$$V_{in} = 162.3 \cdot V_{out}^6 - 492.7 \cdot V_{out}^5 + 587.2 \cdot V_{out}^4 - 346.7 \cdot V_{out}^3 + 103.7 \cdot V_{out}^2 + 668.2 \cdot V_{out} - 1.514 \tag{2.10}$$

When a measurement is performed, the output of the ADC is logged into a CSV file by 20-sim 4C, for later reference.

2.1.6 Leakage resistor

Since the high voltage source can be seen as a large charged capacitor to be able to store as much energy, the time it takes to discharge this capacitor is dependent on the current drawn from it. The resistors in the circuit are all in the order of mega ohms. Thus the current will be negligibly small. To improve the dynamic behaviour of the HV-source, a leakage resistor is added parallel to the sample to allow a maximum leakage current of 10 milliamperes. This leakage resistor then needs to be $R_{leak} = \frac{700\ V}{10 \cdot 10^{-3}\ A} = 70 \cdot 10^3\ \Omega$. However, this resistance will then need to dissipate the power $P_{dis} = 700\ V \cdot 10\ mA = 7\ W$. The resistors available can dissipate 0.4 W. To make this situation possible, the power should be divided over multiple resistors in series. To use resistors that are standard available, 3.3 $k\Omega$ resistors were used. Then the amount of resistors needed is: $\frac{70 \cdot 10^3}{3.3 \cdot 10^3} = 21.2$. Thus, if we use 21 resistors, the amount of power dissipated in each one is: $P_{dis} = i^2 \cdot R = (10 \cdot 10^-3)^2 \cdot 3300 = 0.33\ W$, which is smaller than the specified 0.4 W.

2.1.7 Microscope and video recording

To observe the displacement, a microscope was used. With the microscope it was possible to see displacements in the order of micrometers. To be able to analyse the movement of the sample, the visual data obtained through the microscope is recorded using a video camera mounted on top of the microscope. When the camera has a voltage input of 12 volts, it will output an analog grayscale video signal that is converted through a video grabber to a digital signal, which is saved using a specific software package.

2.1.8 LED signal

Because the input voltage signal and the output video signal are recorded by different software packages, a time synchronisation issue can exist. In order to minimise the shift in time due to this incorrect synchronisation, a visual signal related to the digital signal specified by 20-sim needs to be included. The visual signal will indicate a specific point in time, which can be used to synchronise the two different signals. In order to generate this visual signal, an light emitting diode is built into the safety enclosure directly under the sample, so its output will be visible by the camera's field of view. An electronic signal will be applied via a digital output port of the RaMstix. The electronic signal consists of a square wave for a certain period that is specified to start and stop at a specific time during the experiments. The reflection of the LED's emitted light upon the sample will be visible in the video signal that is recorded.

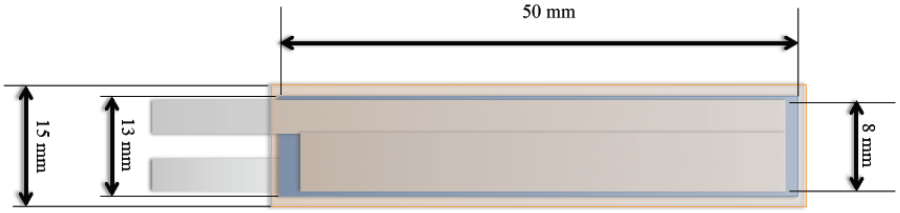

(a) Global dimensions of the piezoelectric sample

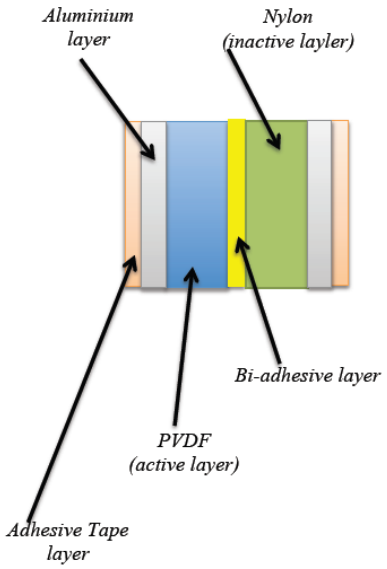

(b) Cross-section of the piezoelectric sample

2.1.9 Piezoelectric sample

The piezoelectric sample is a unimorph active layer glued together with a passive supported layer and wrapped in two layers of aluminium foil as electrodes with tape. The global dimensions and the layout of the sample is visible in figure 2.4a. The cross-section of the sample is displayed in figure 2.4b. The thickness of each successive layer is:

- Active layer $\approx 40\mu m$
- Inactive layer $\approx 20\mu m$
- Bi-adhesive layer $\approx 90\mu m$
- Aluminium layers $\approx 20\mu m$
- Adhesive layers $\approx 45\mu m$

The sample is clamped at 43 millimeters with respect to the tip.

2.2 Experiment plan

2.2.1 Strain measurement

The strain measurement is the application of a large potential to achieve and record a displacement of the tip of the sample. Since this displacement is small for the voltage range applied to the sample, a microscope is needed to record the displacement.

Equipment

- Microscope with 20x optical magnification
- Video recorder compatible with the microscope. This recorder has an RCA output connector.
- Terratec video grabber to convert signal from RCA connector to USB.
- Technix High Voltage generator with remote connection (0-700V)
- Amplifier circuit
- RaMstix FPGA board

- Sample mount and safety enclosure
- Samples
- Laptop with 20-sim and Terratec software
- Matlab software for video analysis

Method

A predefined signal is applied with the FPGA board using the 20-sim software to the amplifier, which modulates the High Voltage generator accordingly. By measuring the transfer functions of the respective stages beforehand, the applied signal can be planned to a reasonable accuracy. Furthermore, the applied signal is looped back into the FPGA board through a voltage divider to check the applied signal. The response of the sample is recorded and can be analysed afterwards.

Applied signals

These signals will be applied to all samples. See figure 2.5

- Step function from 0 to 700 volts with steps of 100 volts for a constant time-step T, after which the signal goes to 0 and the unloading is recorded as well for a constant period of time. The parameters time-step, voltage step and maximum voltage can be varied with each measurement.
- Ramp function from 0 to 700 volts with a slope of 100 volts per time-step T, after which the signal goes to 0 and the unloading is recorded as well for a constant period of time. The parameters slope and maximum voltage can be varied.
- Symmetric ramp function which linearly increases from 0 to 700 volts with a slope of 100 volts per time-step T, after which the signal stays constant for a moment and then decreases with the same slope. The parameters slope, maximum voltage and stationary time can be varied.
- Sinusoid function which oscillates for a specified period of time with a certain offset and amplitude. The total oscillation period, the offset, the amplitude and the frequency can be varied. The signal should stay between 0 and 700 volts.
- Square wave function which oscillates for a specified period of time with a certain offset and amplitude. The total oscillation period, the offset, the amplitude and the frequency can be varied. The signal should stay between 0 and 700 volts.
- Sawtooth wave function which oscillates for a specified period of time with a certain offset and amplitude. The total oscillation period, the offset, the amplitude and the frequency can be varied. The signal should stay between 0 and 700 volts.

Performed measurements

- Step function (100 V step to 700 V)
  - T=10s
  - T=30s
  - T=180s
- Step function (100 V step to 500 V)
  - T=10s
  - T=180s
- Step function (175 V step to 700 V)
  - T=180s
- Ramp function (100 V slope to 700 V)
  - T=10s

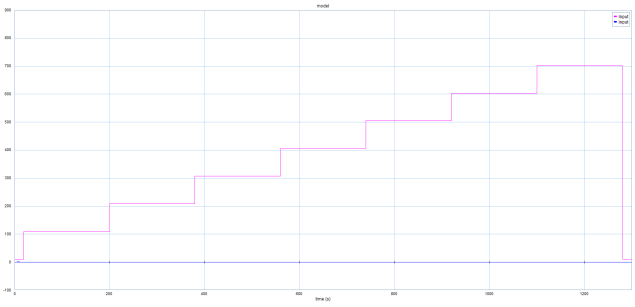

(a) Step function

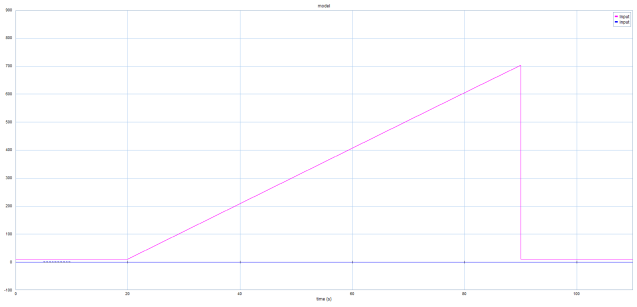

(b) Ramp function

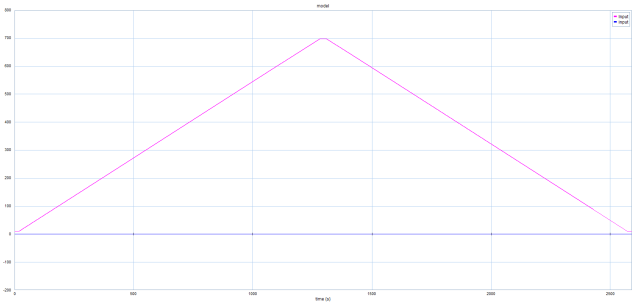

(c) Symmetric ramp function

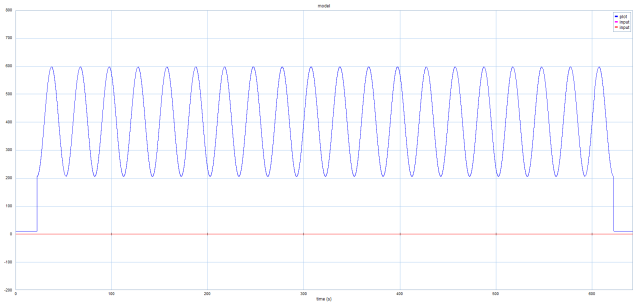

(d) Sine wave function

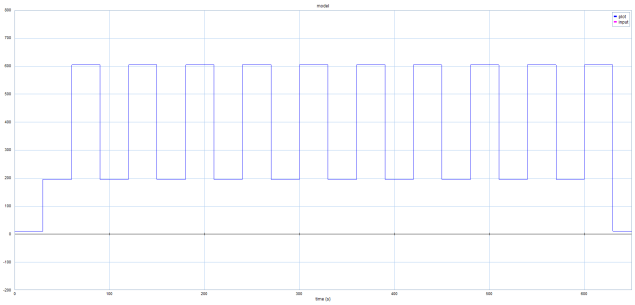

(e) Square wave function

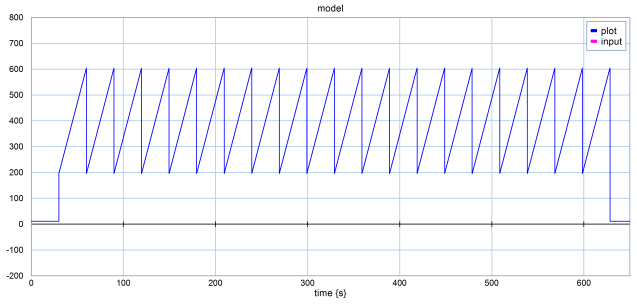

(f) Sawtooth wave function

Figure 2.5: Applied signals

  - T=30s
- Ramp function (50 V slope to 360 V)
  - T=180s
- Symmetric ramp function (100 V slope to 700 V)
  - T=10s
  - T=30s
- Sine wave function (200 to 600 volts peak to peak for 600 seconds)
  - 10 revolutions
  - 20 revolutions
  - 100 revolutions
- Square wave function (200 to 600 volts peak to peak for 600 seconds)
  - 10 revolutions
  - 20 revolutions
  - 100 revolutions
- Sawtooth wave function (200 to 600 volts peak to peak for 600 seconds)
  - 20 revolutions
- Reversed polarity symmetric ramp function (100 V slope to 700 V)
  - T=30s
- Reversed polarity sine wave function (200 to 600 volts peak to peak for 600 seconds)
  - 20 revolutions

All measurements were followed by 600 seconds recording the relaxation of the sample.

Analysis of the results

The displacement of the tip of the is recorded with a video camera mounted on the microscope. The recorded video data will be analysed using a custom made Matlab script, which will track the tip and relay its extracted data into a CSV file.

2.2.2 Resonance measurement

The goal is to find the electrical resonance point, as it could be an indication of the mechanical properties. Therefore, the resonance point should change with increasing applied (constant) voltage.

The change in electrical impedance of a material is related to internal structural changes. Therefore, the electrical resonance point can indicate the mechanical resonance frequency of the material. This resonance frequency can be related to the mechanical stiffness of the material by equation 1.2.

Equipment

- Series resistance
- HV generator
- Amplifier circuit
- RaMstix
- PC with 20-sim software
- Samples
- Sample mount and safety enclosure

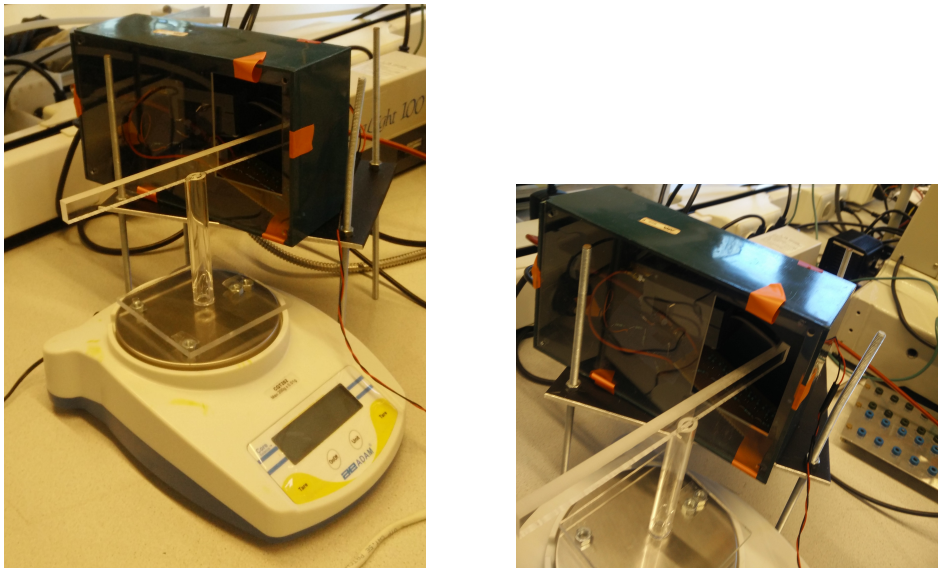

Figure 2.6: The balance set-up to measure the force exerted by the sample

Method

To analyse the impedance variation with respect to the frequency, a resistor is placed in series with the sample. The current through the sample is regulated by its impedance, so the voltage divider created by placing the resistor in series, and measuring the voltage drop across the resistor, gives an indication of the impedance of the sample. Because the voltage drop across the resistor should be measurable, the resistance of the resistor needs to be very large. Therefore, the resistance is chosen to be 19.75 $M\Omega$.

2.2.3 Force measurement

The goal is to measure the force exerted by a sample on a mechanical construction with a balance.

Equipment

- Mechanical construction
- Adam Equipment CQT202 Core Compact Portable Balance
- Samples
- Sample mount and safety enclosure
- Lift stage
- HV generator
- Amplifier circuit
- RaMstix
- PC with 20-sim software

The samples will press with the tip against the mechanical construction, which will result in a small downwards force, which is converted into a numerical value by the balance. The balance has a repeatability error of 0.02 grams or 0.0002 N or 0.2 mN.[4] See figure 2.6. The safety enclosure is placed on a lift stage to reach the desired height. The mechanical construction consists of a horizontal beam of 20 centimetres glued in the middle on top of a cylinder of 10 centimetres which is glued in the middle on top of a square base of 8 by 8 centimetres. To ensure that the base will not roll, small cylinders (nuts) are attached to the bottom to provide a 3-point contact to increase stability.

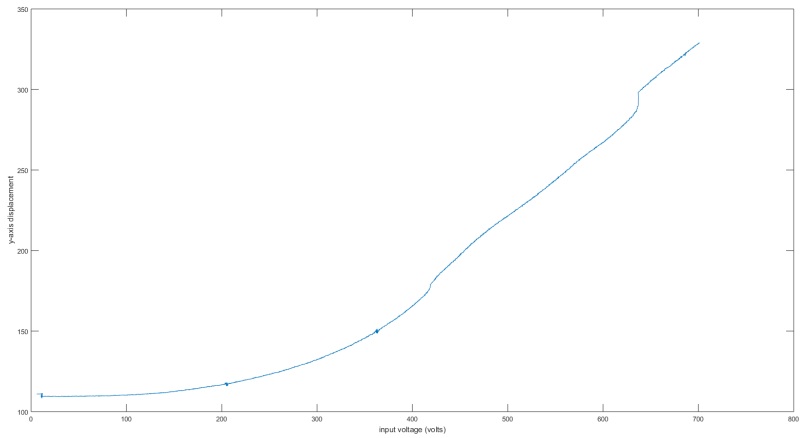

Figure 2.7: y-axis displacement response as a function of voltage

2.3 Results

2.3.1 Strain measurement

The script used to extract the position data from the video files is included in appendix B. The script is an extension of a Mathworks example used for tracking a face.[9] It uses a Kanade-Lucas-Tomasi (KLT) algorithm to track the movement of points of interest. These points of interest are extracted from the first frame by specifying a region of interest. Inside this region a minimum eigenvalue algorithm detects corners based on the gradients of the intensity of the grayscale frame. The movements of these corner points are then tracked for each successive frame until the end of the video. This data is exported into a matrix that is stored into a "comma separated value" file, that can be easily imported again for post-processing and analysis.

Unfortunately, because the quality of the video data is not high, the tracker is not completely stable. The algorithm can lose track or shift along a ridge in the photo, because the gradient does not change much. So, the result still has to be checked for its validity. From the output data you can see quickly when a point has lost track, because it will become a constant value. And the tracking is streamed in a video player, so you can see how much the point shifts in the video. Based on that, the validity of tracking data can be qualitatively determined.

Independent of the accuracy, the results should still prove to be useful, as the general behaviour should still be visible in the plot shape. The specific fit values will differ, but the general conclusions will remain the same.

All of the strain results are displayed in appendix C. The minimum qualitative accuracy is around 93% relative to the amplitude of the response.

Based on the strain response of the 30 seconds period ramp input, a y-axis displacement as a function of voltage is plotted in figure 2.7 as an indication of the relationship.

To compare this result to literature data, the values are converted to strain as a function of electric field, which is displayed in figure 2.8

The strain response is fitted to a quadratic polynomial fit, as that behaviour is expected from the electrostrictive model. See figure 2.9.

The quadratic fit yields the result of the quadratic function, with an R^2 value of 0.9963:

$$S(E) = 0.09715 \cdot E^2 + 0.2251 \cdot E + 0.1196 \tag{2.11}$$

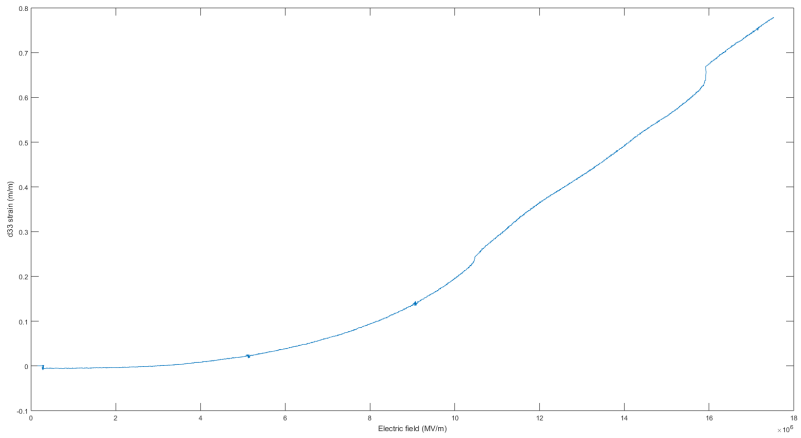

Figure 2.8: d_{33} strain response as a function of electric field

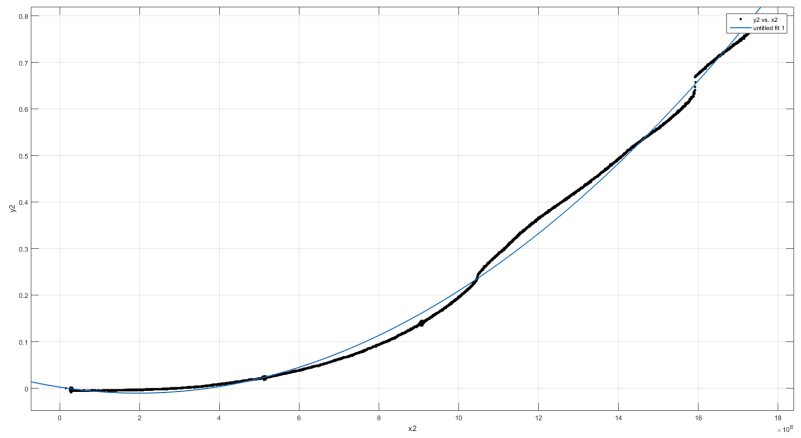

Figure 2.9: Quadratic fitting of strain response

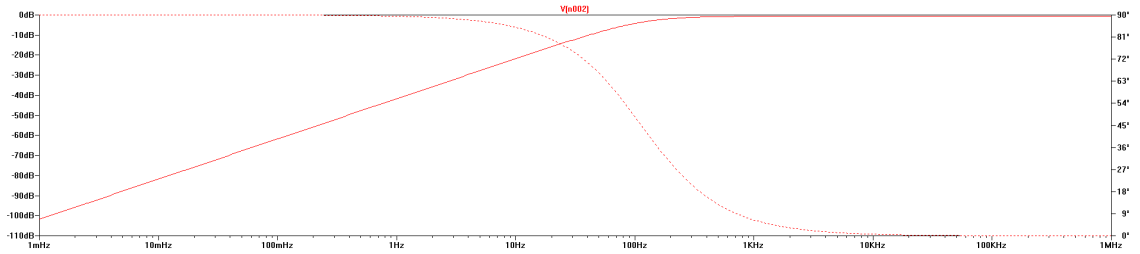

Figure 2.10: The theoretical frequency response of the high pass filter created by the sample

2.3.2 Resonance measurement

The proposed electrical network has been built and adapted to make it interchangeable with the original circuit. The results however, show a number of limiting issues.

1. The capacitance of the sample in series with the resistance create a passive high-pass CR filter with a breakpoint frequency of about 122 Hz. Therefore, the transfer for the low frequencies influences the measurement. See the theoretical frequency response in figure 2.10.
2. The high-voltage generator has a capacitive behaviour, which means the derivative of the voltage is dependent on the current drawn. This current is currently limited around 10 mA, which enables a maximum $\frac{dV}{dt} \approx 407.56\ \frac{V}{s}$.
3. A lot of noise exists in the system. Due to unknown sources, there exists a band of high-frequency noise with an amplitude of about 0.5 V, while the maximum input amplitude of the ADC is 2.5 V. This forms a barrier to conduct the experiment.

To design a suitable experiment that minimises the issues described above, a simple experiment is performed to find the resonance point for the sample material without a DC bias applied. To this end, a signal is applied to the sample with a frequency generator. The signal consists of a sine with a peak-to-peak value of 20 volts. Then the response, i.e. the voltage drop over the series resistor, is measured using an oscilloscope. Since the oscilloscope has an input impedance of 10 mega ohms, it is in the same order of magnitude as the resistor and will also have an influence on the filter behaviour such that it raises the breakpoint frequency to around 363 Hz. With a set of 37 measurement points, a bode plot was made to visualise the actual response of the sample. This is visible in figure 2.11. This bode plot shows no significant resonance frequency.

To ensure that this result is accurate, a HP 3562A Dynamic Signal Analyzer is used to display the frequency spectrum of the sample. With a random noise input provided by the analyzer, the spectrum from 0.1 Hz to 50 kHz is investigated. This range showed only a peak at 50 Hz, which could be contributed to interference from the power mains. Therefore, this result supports the results of the manually made frequency spectrum.

2.3.3 Force measurement

The proposed measurement using the balance yielded a result of 0 N. Increasing the elevation of the lift stage to decrease the initial mechanical loading of the sample also yielded a result of 0 N.

From the design of this measurement, questions regarding the accuracy arise. To address these questions, a simplistic test is used. To check if the internal dissipation of the mechanical structure is having a significant influence on the result, a small mass is placed upon the tip of the structure, which is placed upon the balance to see the weight of the mass. Then the mechanical structure is removed and the small mass is weighed without anything in between. If there is any visible difference in results between the two weighings, the mechanical structure has a significant influence on the experiment.

The result of this test showed no discrepancy in weight between the two measurements. Therefore, it can be concluded that the measurement is accurate up to the resolution of the balance.

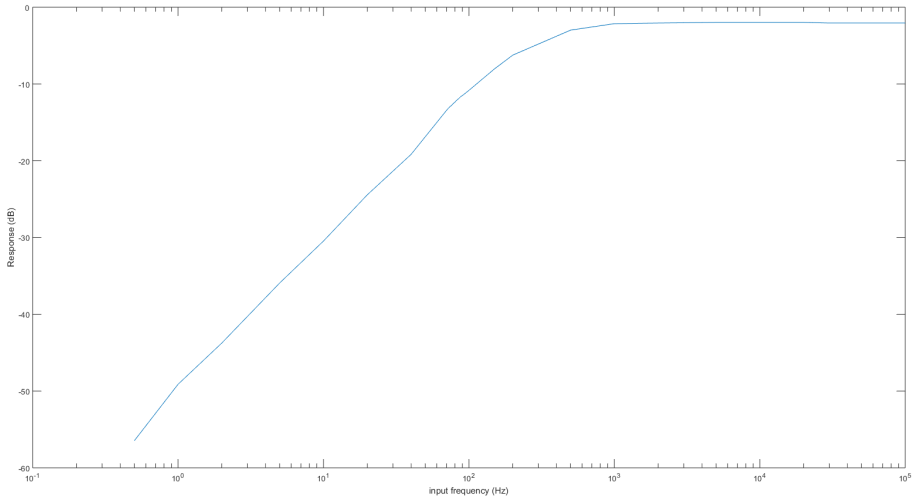

Figure 2.11: The actual frequency response of the high pass filter created by the sample

Conclusions and Discussion

The strain results displayed in appendix C show a general behaviour for specific inputs. The behaviour in time for a step input resembles an exponential increase of the form $f(x) = 1 - e^{-x}$. However, an accurate fit has not been found. This behaviour looks similar to an overdamped system step response. The behaviour in time for a ramp input shows an initial quadratic like increase until it passes a threshold where the behaviour changes to a linear increase with a matching slope to the input. In the T=30s response, a third behaviour change is visible, where it suddenly makes a shift, decreasing the delay of the response introduced by the quadratic start-up. These changes in behaviour could be attributed to phase changes described in the theoretical background part. Additionally, if the change in voltage is significant, like the voltage drop at the end of the ramp input, the material is able to change its movement rapidly. For the relaxation part, the behaviour also shows an decreasing exponential behaviour in time. However, when the amplitude approaches the equilibrium position, the influence of the viscous damping effects of the glue and tape of the sample increases rapidly and the decay slows down dramatically. To reach the equilibrium position, the sample has to be in rest for an extended period of time, that is orders of magnitude larger than any experiment or operating conditions. It is even possible that the material slows down so much that stiction takes over and the material reaches a new equilibrium position.

One additional result that has to be accounted for in practical applications is the independence of the response with respect to the polarity of the applied electric field. This effect has not been tested extensively, but this could mean that there is no means of accelerating the decrease of the strain.

The frequency spectrum of the sample shows no significant resonance frequency. The resonance frequency is related to a ratio between the mechanical stiffness and the mass. As the sample is small, and the polymer material is relatively soft, the mechanical stiffness and the mass are both negligibly small. It is possible that these characteristics are insignificant compared to the dominant behaviour aspects of the material. However, no accurate conclusions can be made based upon these results.

The force exerted by the sample is smaller than the measuring range of the balance, which is 0.2 millinewtons. This result can be expected as the weight of the sample is only a few grams. Of this sample, only a fraction is the active material. Therefore, if the force exerted would be measurable by this experiment, the active material would have to exert a force greater than its own weight.

Discussion

The results do not have a definite accuracy, which is something that should be improved in further research. Determining the accuracy of the results is difficult for the designed set-up, but conclusions can be made about the general behaviour of the material. Furthermore, relevant data has been lost due to administrative issues in combination with the repetitive behaviour of the experiment. Therefore, one has to be careful to keep track of the process steps.

Bibliography

[1] Valentina Cauda, Giancarlo Canavese, and Stefano Stassi. Nanostructured piezoelectric polymers. *Journal of Applied Polymer Science*, 132, April 2015.

[2] Z.-Y. Cheng, V. Bharti, T.-B. Xu, Shexi Wang, Q. M. Zhang, T. Ramotowski, F. Tito, and R. Ting. Transverse strain responses in electrostrictive poly(vinylidene fluoride-trifluoroethylene) films and development of a dilatometer for the measurement. *Journal of Applied Physics*, 86:2208–2214, August 1999.

[3] Z.-Y. Cheng, V. Bharti, T.-B. Xu, Haisheng Xu, T. Mai, and Q.M. Zhang. Electrostrictive poly(vinylidene fluoride-trifluoroethylene) copolymers. *Sensors and Actuators A*, 90:138–147, 2001.

[4] Adam Equipment. Cqt 202 core compact portable balance. `http://www.adamequipment.com/am/details/178/337`.

[5] Matteo Fumagalli, Eamon Barrett, Stefano Stramiglioli, and Raffaela Carloni. The mvsa-ut: a miniaturized differential mechanism for a continuous rotational variable stiffness actuator. In *4th IEEE RAS & EMBS International Conference on Biomedical Robotics and Biomechatronics*, pages 1943 – 1948. IEEE, June 2012.

[6] Shishang Guo, H.L.W. Chan, X.-Z. Zhao, and C.L. Choy. Factors affecting the performance of the bimorph-based dilatometer for field induced strain measurement of polymer films. *Review of Scientific Instruments*, 74(3), March 2003.

[7] Cheng Huang, R. Klein, Feng Xia, Hengfeng Li, Q.M. Zhang, François Bauer, and Z.-Y. Cheng. Poly(vinylidene fluoride-trifluoroethylene) based high performance electroactive polymers. *IEEE Transactions on Dielectrics and Electrical Insulation*, 11(2):299–311, April 2004.

[8] William D. Callister Jr. and David G. Rethwisch. *Fundamentals of Materials Science and Engineering*. John Wiley & Sons, Inc., 3rd edition, 2008.

[9] Mathworks. Track points in video using kanade-lucas-tomasi (klt) algorithm. `http://nl.mathworks.com/help/vision/ref/vision.pointtracker-class.html`.

[10] P. Muralt. Stress coupled phenomena: Piezoelectric effect. In K.H. Jrgen Buschow, Robert W. Cahn, Merton C. Flemings, Bernhard Ilschner, Edward J. Kramer, Subhash Mahajan, and Patrick Veyssire, editors, *Encyclopedia of Materials: Science and Technology*, pages 8894 – 8897. Elsevier, 2nd edition, 2001.

[11] J. Su, P. Moses, and Q.M. Zhang. A bimorph based dilatometer for field induced strain measurement in soft and thin free standing polymer films. *Review of Scientific Instruments*, 69, 1998.

[12] Technix, 8, rue Eugne Dupuis, 94 000 CRETEIL France. *DC High Voltage Generators 300 W to 3 kW SR Series*. `http://www.technix-hv.com/technix/sites/default/files/downloads/DATASHEET_SR-300-3000-W-SERIES_ENG.pdf`.

Appendices

A. Data fit figures

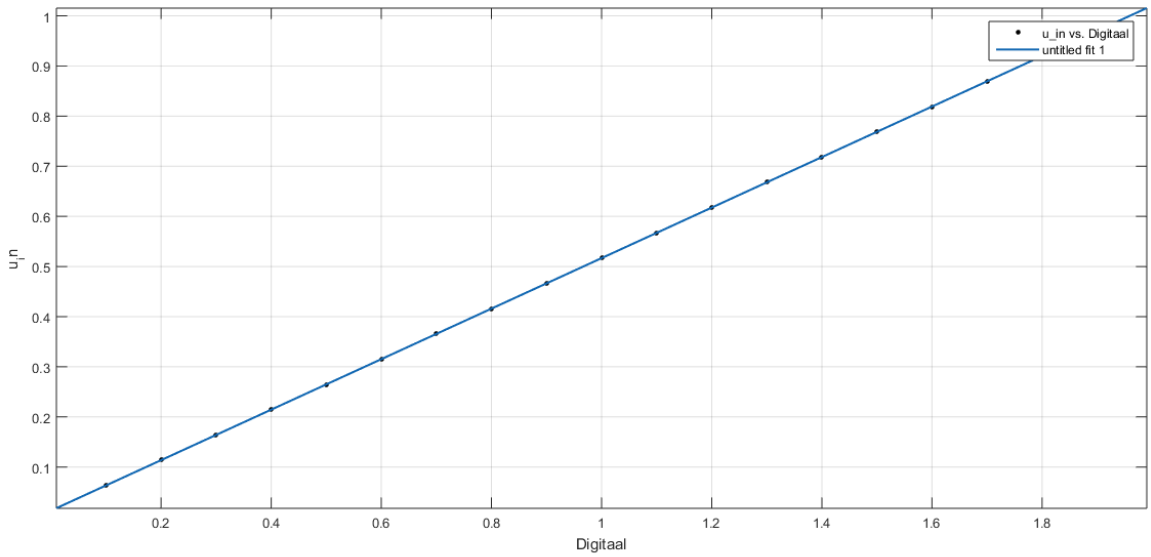

Figure A.1: Linear fit of measurements transfer digital signal to output DAC

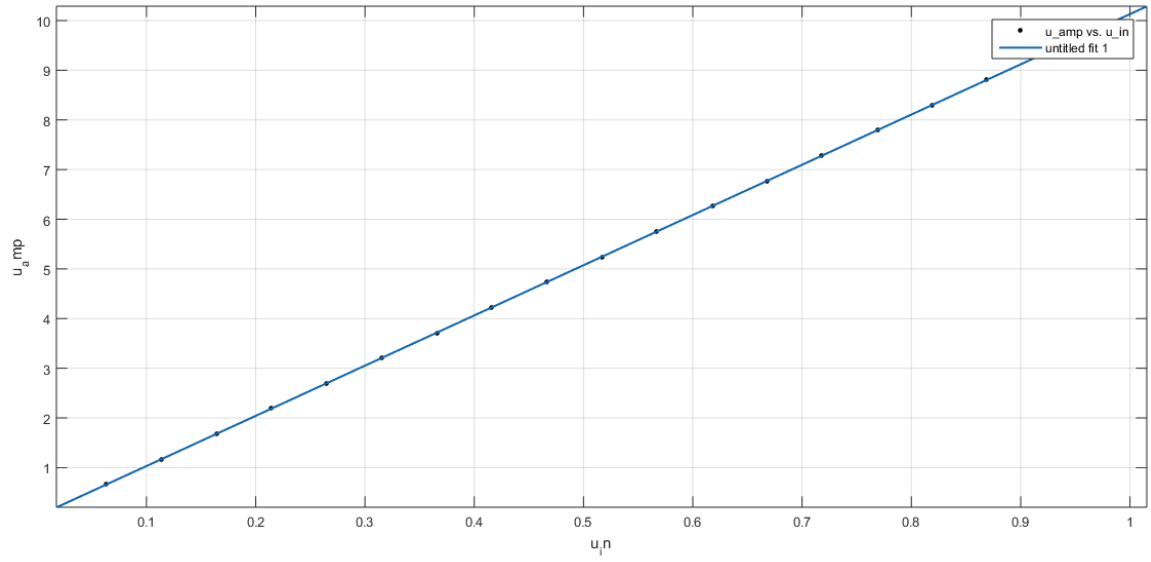

Figure A.2: Linear fit of measurements transfer amplifier stage input to output

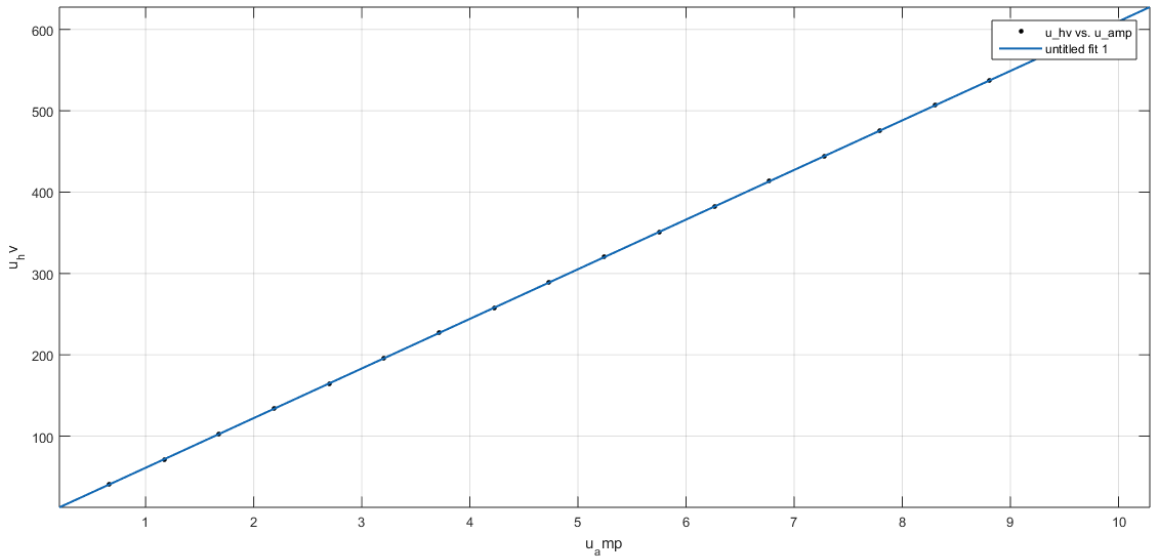

Figure A.3: Linear fit of measurements transfer amplifier stage output to the output of the high voltage generator

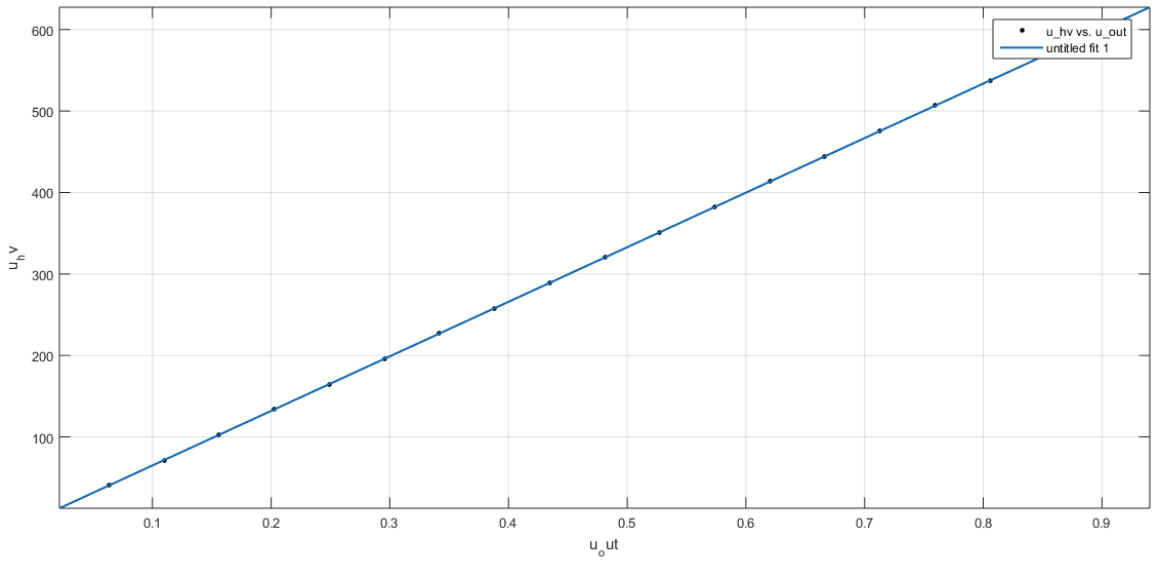

Figure A.4: Linear fit of measurements transfer output of the high voltage generator to the output of the ADC

B. Matlab point tracker script

```
clear variables
close all
clc
inputname = 'RampT180/RampT180.mp4';
profile = 'MPEG-4';

videoFileReader = vision.VideoFileReader(inputname);
videoPlayer = vision.VideoPlayer('Position', [100, 100, 680, 520]);

objectFrame = step(videoFileReader);
objectRegion = [420, 392, 15, 15];

objectImage = insertShape(objectFrame, 'Rectangle', objectRegion, 'Color', 'red');
figure;
imshow(objectImage);
title('Red box shows object region');

points = detectMinEigenFeatures(rgb2gray(objectFrame), 'ROI', objectRegion);

pointImage = insertMarker(objectFrame, points.Location, '+', 'Color', 'white');
figure, imshow(pointImage), title('Detected interest points');

tracker = vision.PointTracker('MaxBidirectionalError', 1);
initialize(tracker, points.Location, objectFrame);

timecounter = 1;

while ~isDone(videoFileReader)
      frame = step(videoFileReader);
      [points, validity] = step(tracker, frame);
      out = insertMarker(frame, points(validity, :), '+');
      step(videoPlayer, out);

      x1points(timecounter)=points(1);
      y1points(timecounter)=points(2);

      timecounter = timecounter+1;
end

release(videoPlayer);
release(videoFileReader);

time = linspace(0, length(xpoints)/24,length(xpoints));
M = [time; x1points; y1points];
csvwrite(strcat(inputname,'.csv'),M)
```

C. Strain result plots

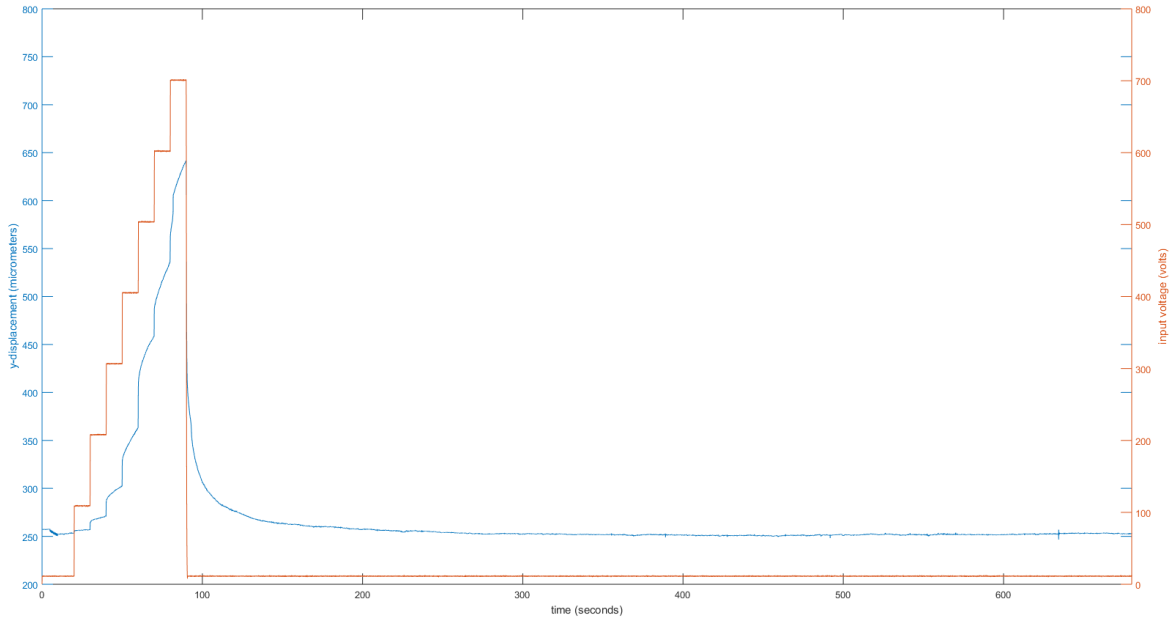

Figure C.1: The y-axis strain response for a 100 V step input until 700 V for T=10 seconds

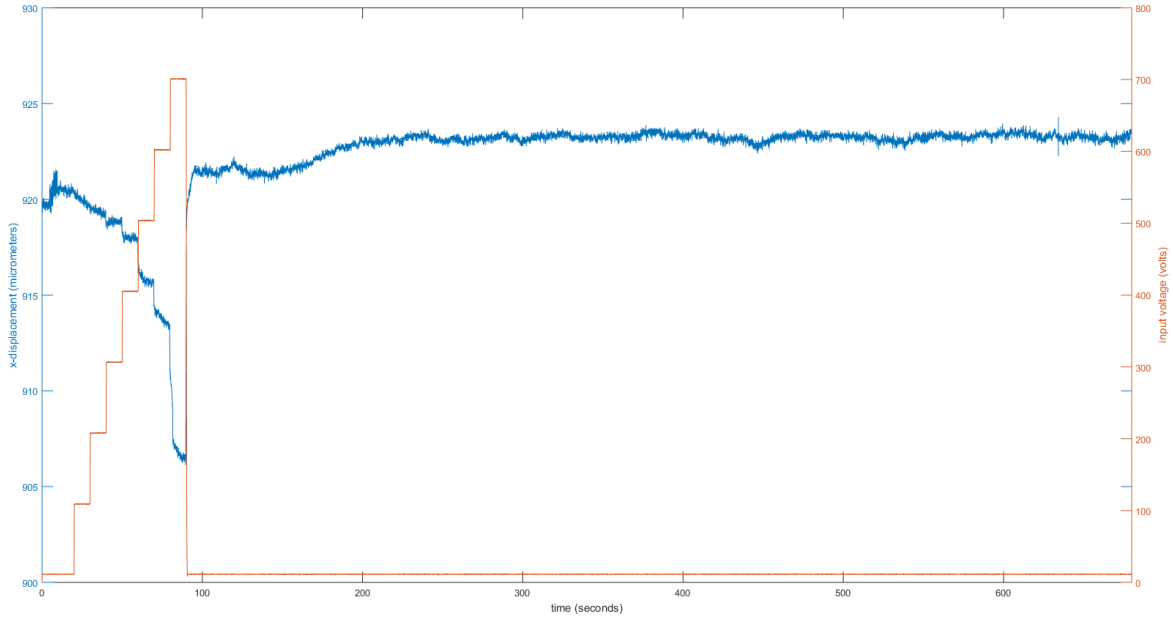

Figure C.2: The x-axis strain response for a 100 V step input until 700 V for T=10 seconds

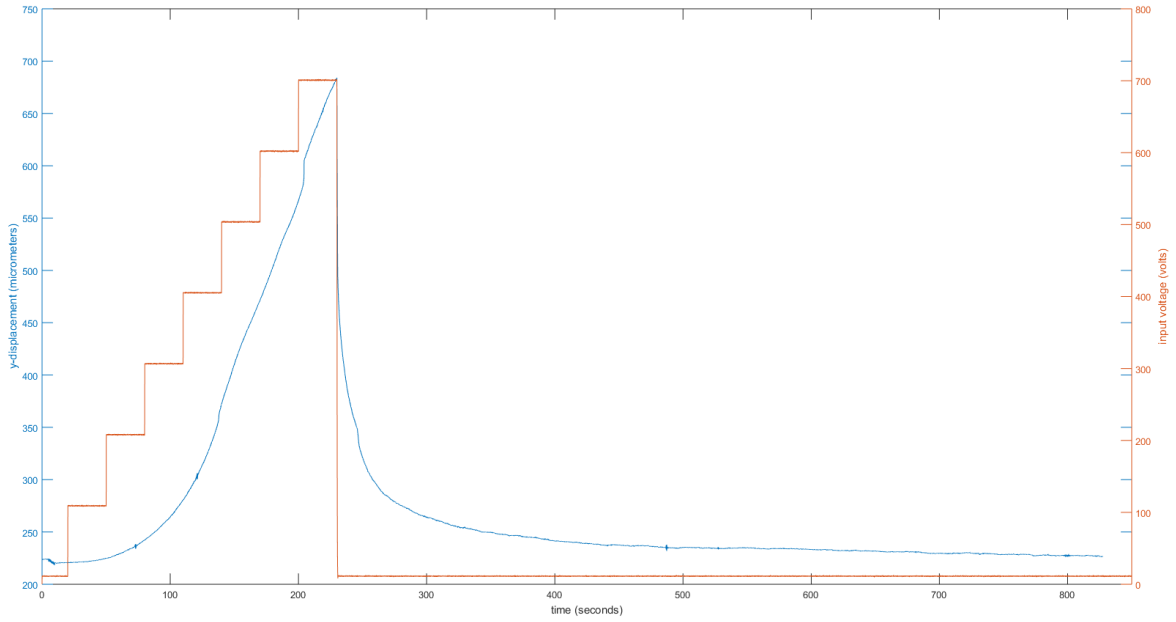

Figure C.3: The y-axis strain response for a 100 V step input until 700 V for T=30 seconds

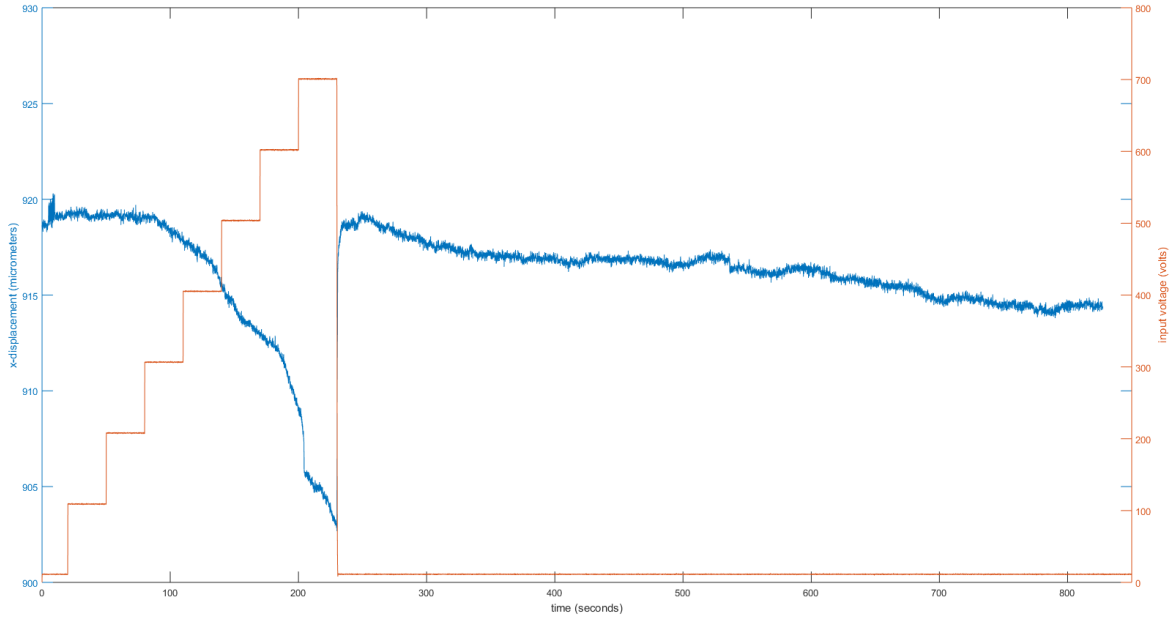

Figure C.4: The x-axis strain response for a 100 V step input until 700 V for T=30 seconds

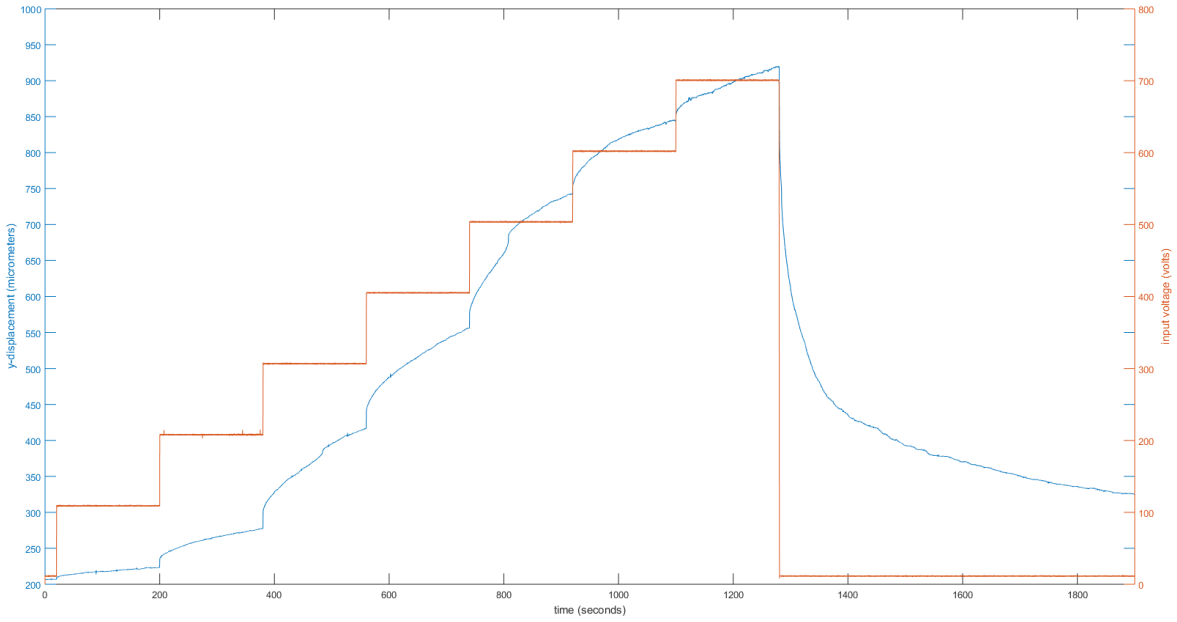

Figure C.5: The y-axis strain response for a 100 V step input until 700 V for T=180 seconds

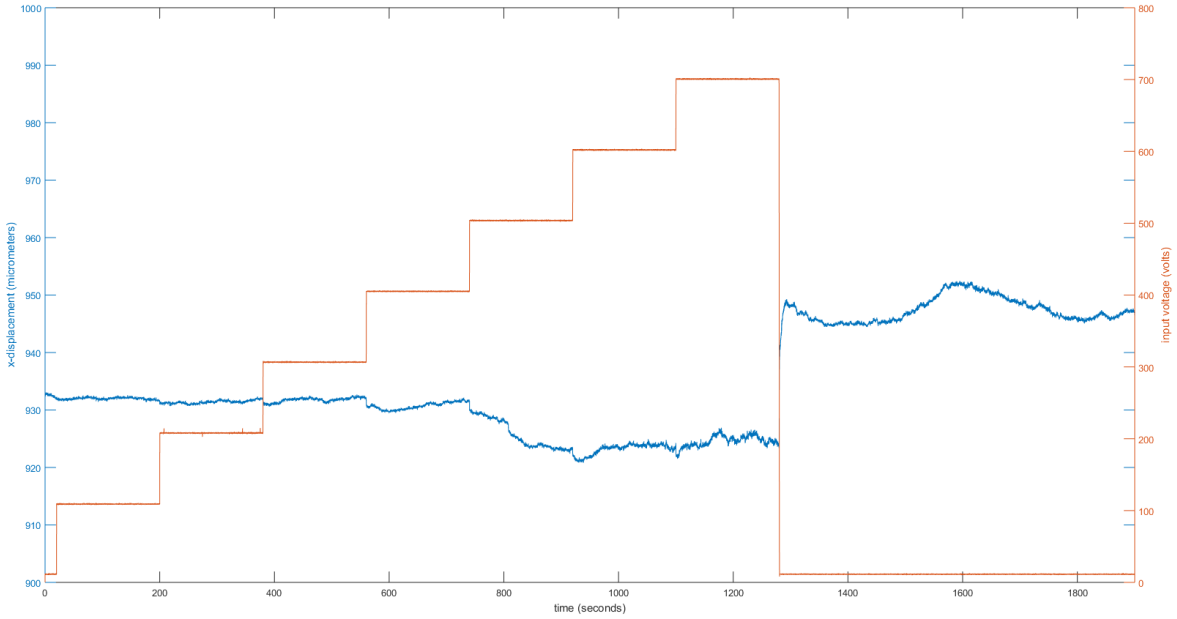

Figure C.6: The x-axis strain response for a 100 V step input until 700 V for T=180 seconds

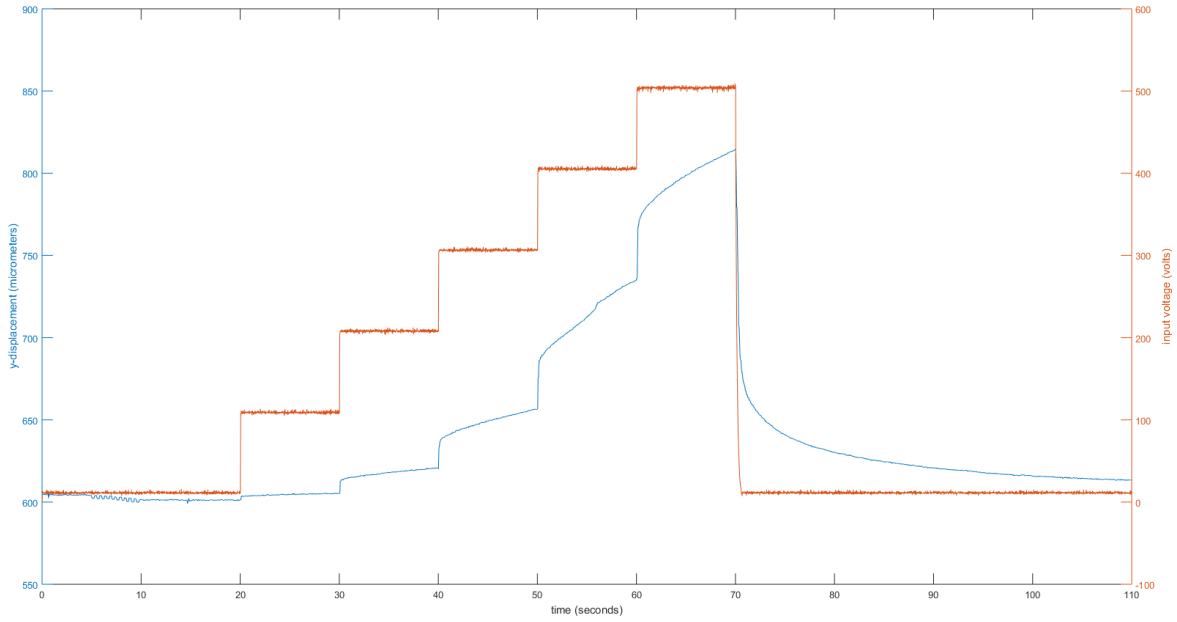

Figure C.7: The y-axis strain response for a 100 V step input until 500 V for T=10 seconds

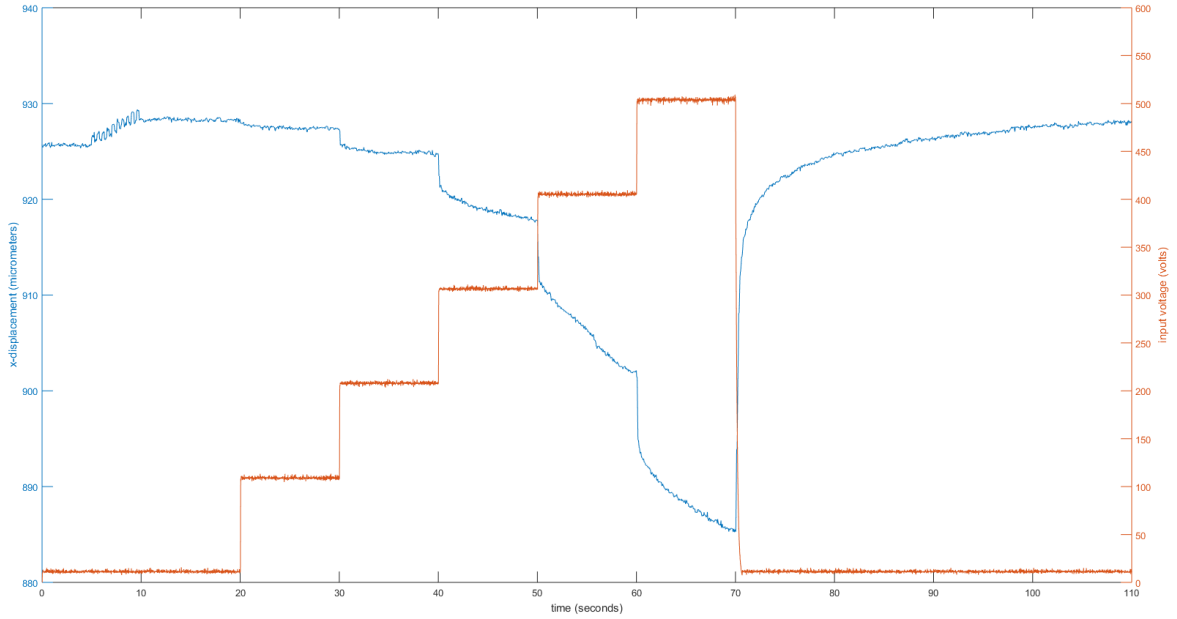

Figure C.8: The x-axis strain response for a 100 V step input until 500 V for T=10 seconds

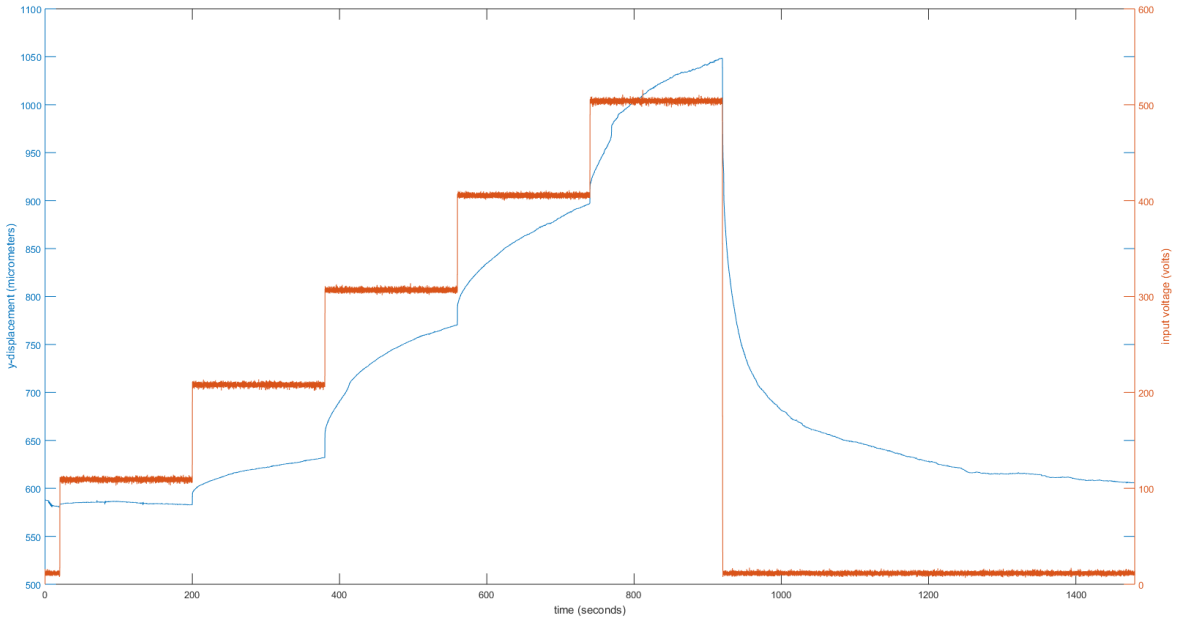

Figure C.9: The y-axis strain response for a 100 V step input until 500 V for T=180 seconds

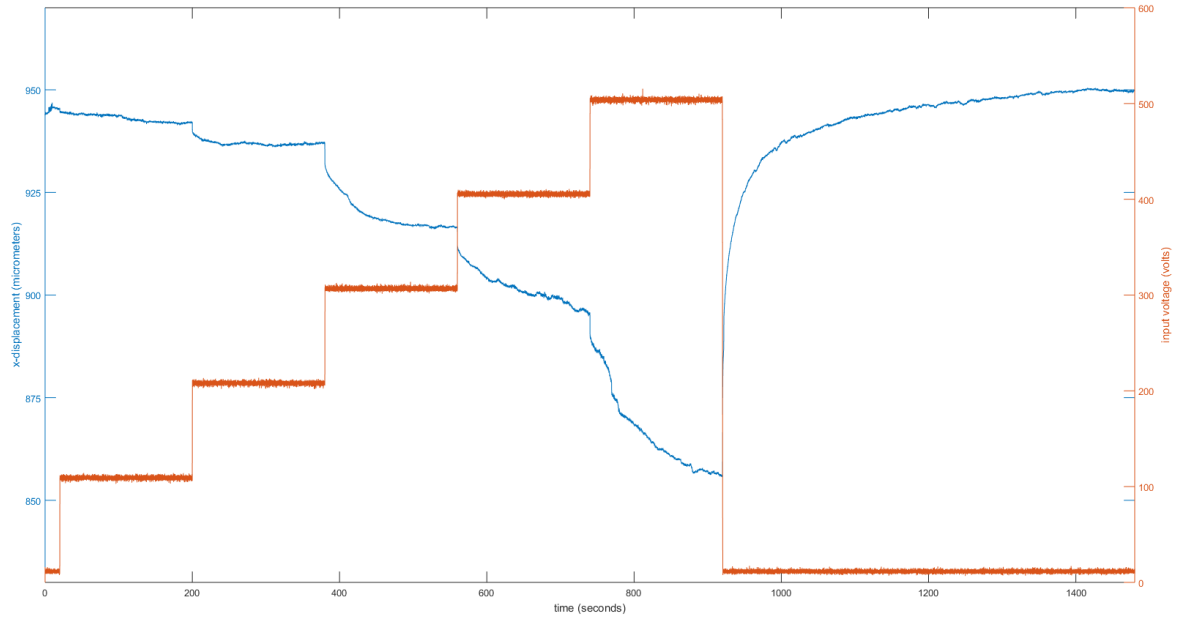

Figure C.10: The x-axis strain response for a 100 V step input until 500 V for T=180 seconds

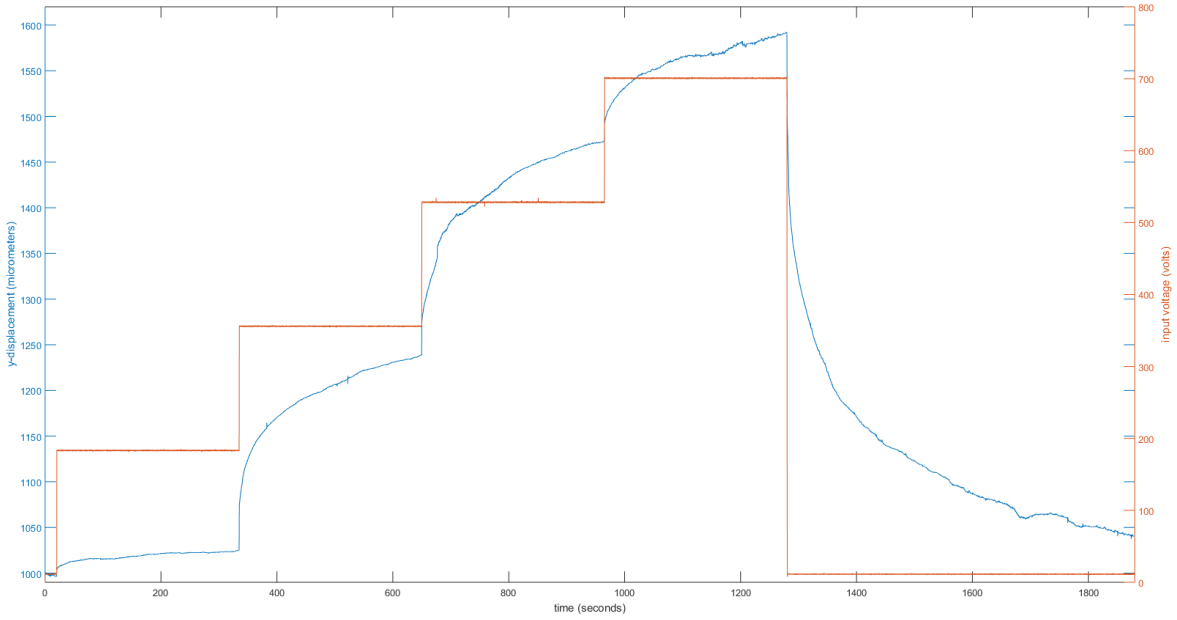

Figure C.11: The y-axis strain response for a 175 V step input until 700 V for T=180 seconds

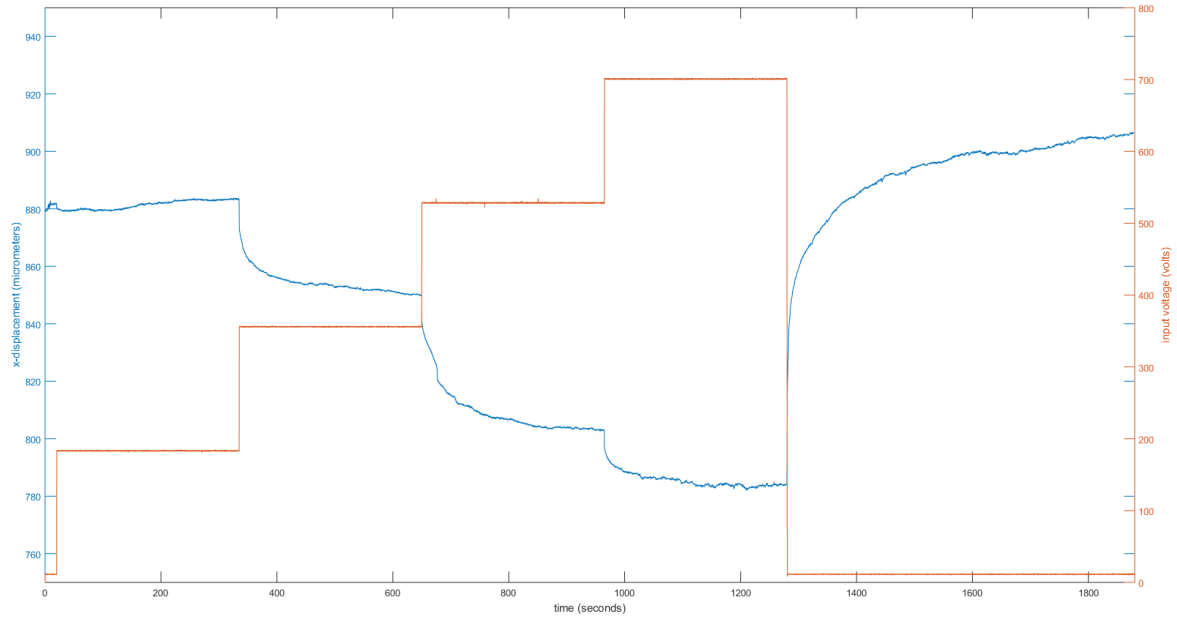

Figure C.12: The x-axis strain response for a 175 V step input until 700 V for T=180 seconds

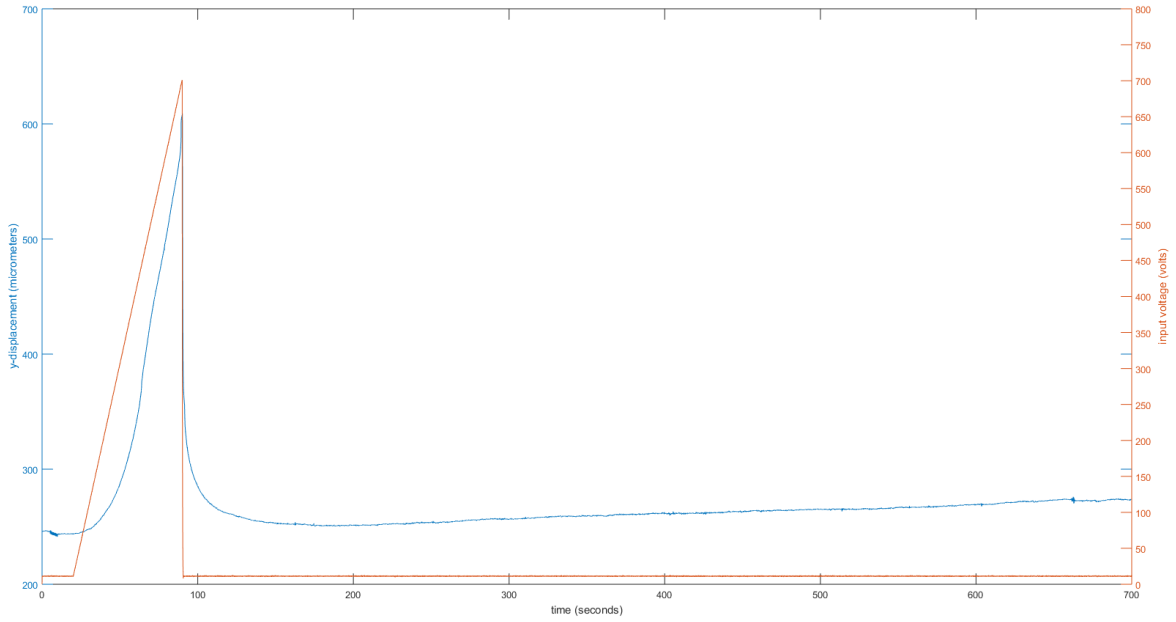

Figure C.13: The y-axis strain response for a 100 V ramp input until 700 V for T=10 seconds

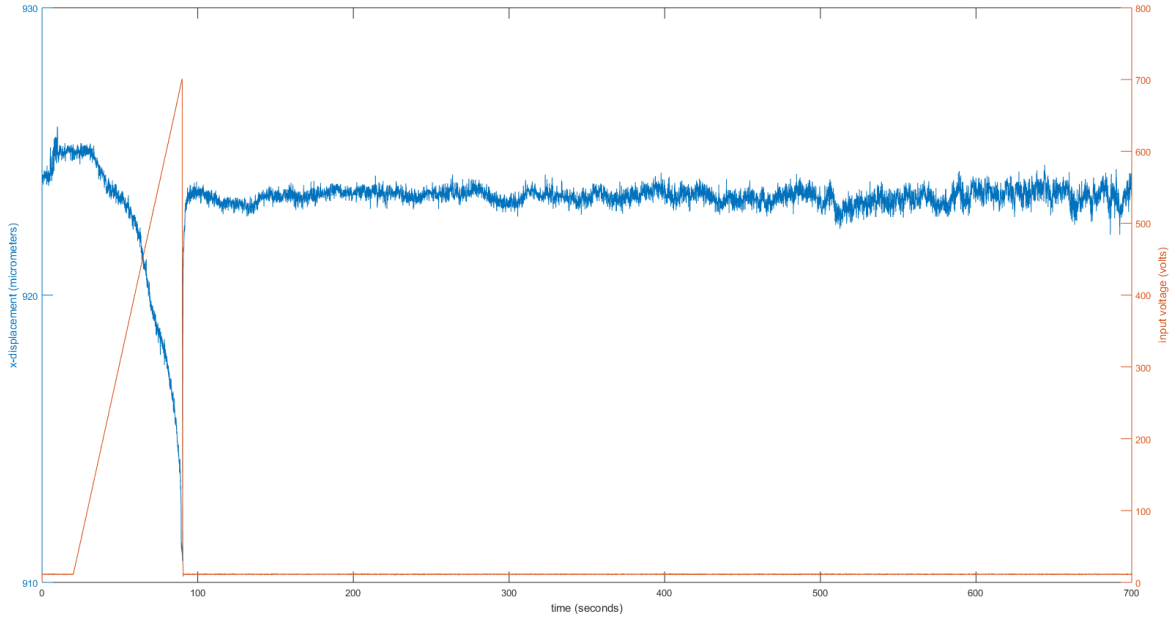

Figure C.14: The x-axis strain response for a 100 V ramp input until 700 V for T=10 seconds

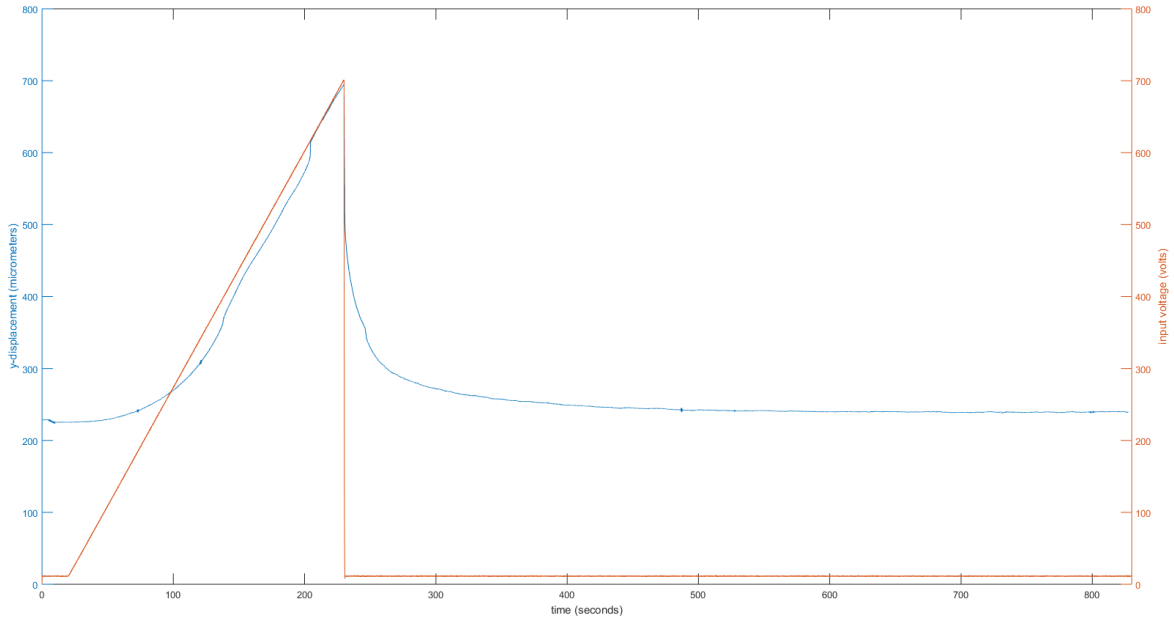

Figure C.15: The y-axis strain response for a 100 V ramp input until 700 V for T=30 seconds

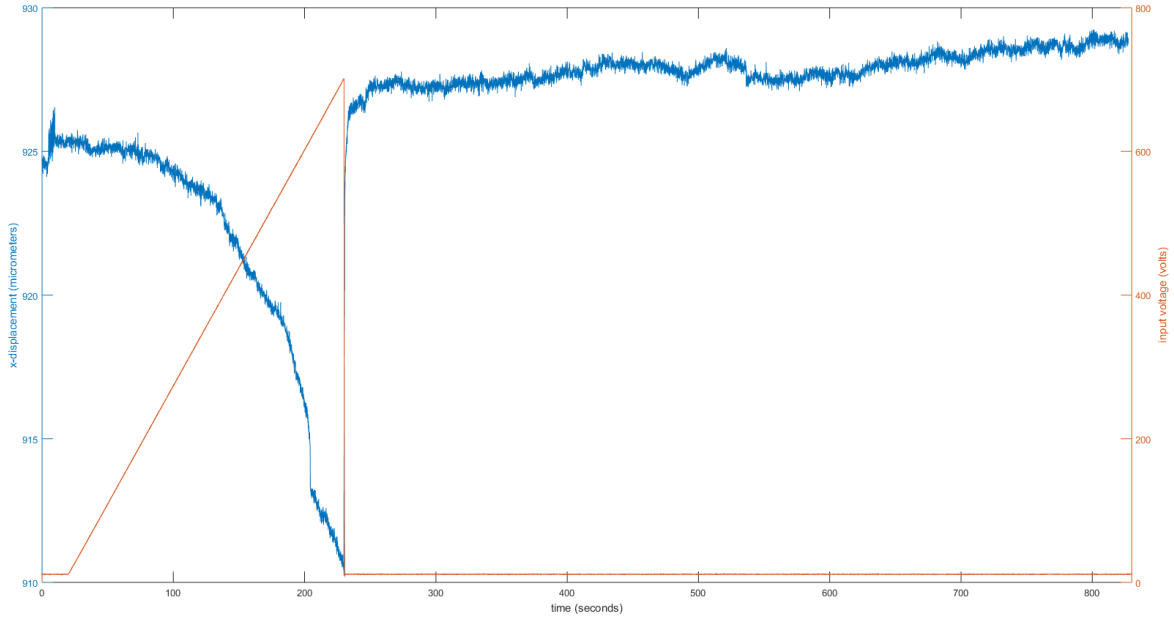

Figure C.16: The x-axis strain response for a 100 V ramp input until 700 V for T=30 seconds

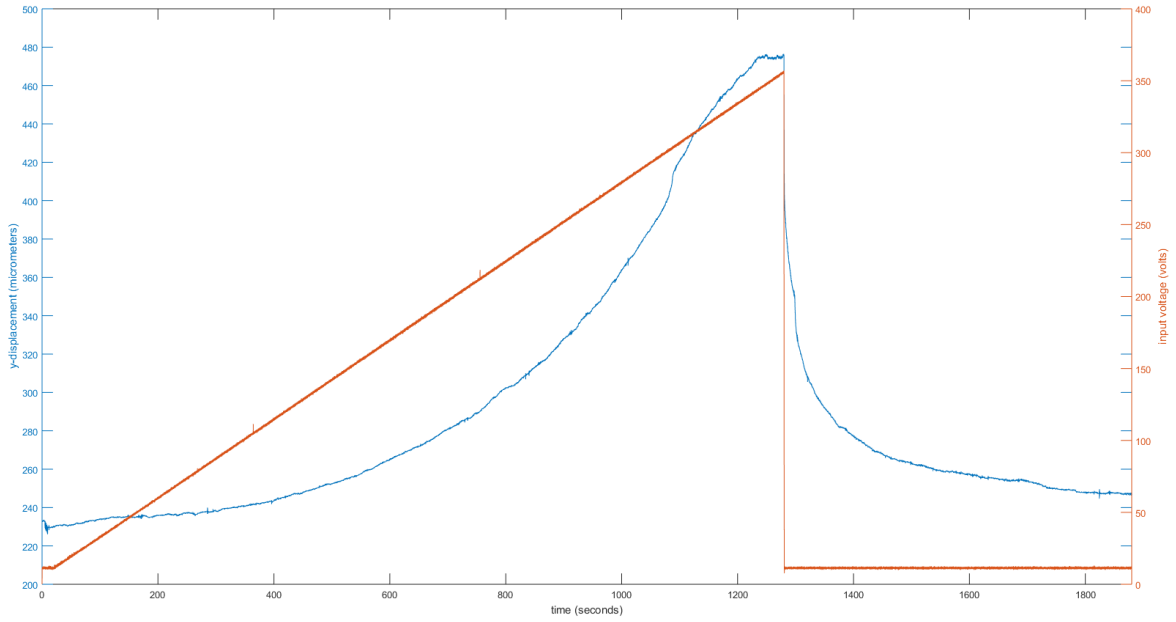

Figure C.17: The y-axis strain response for a 50 V ramp input until 360 V for T=180 seconds

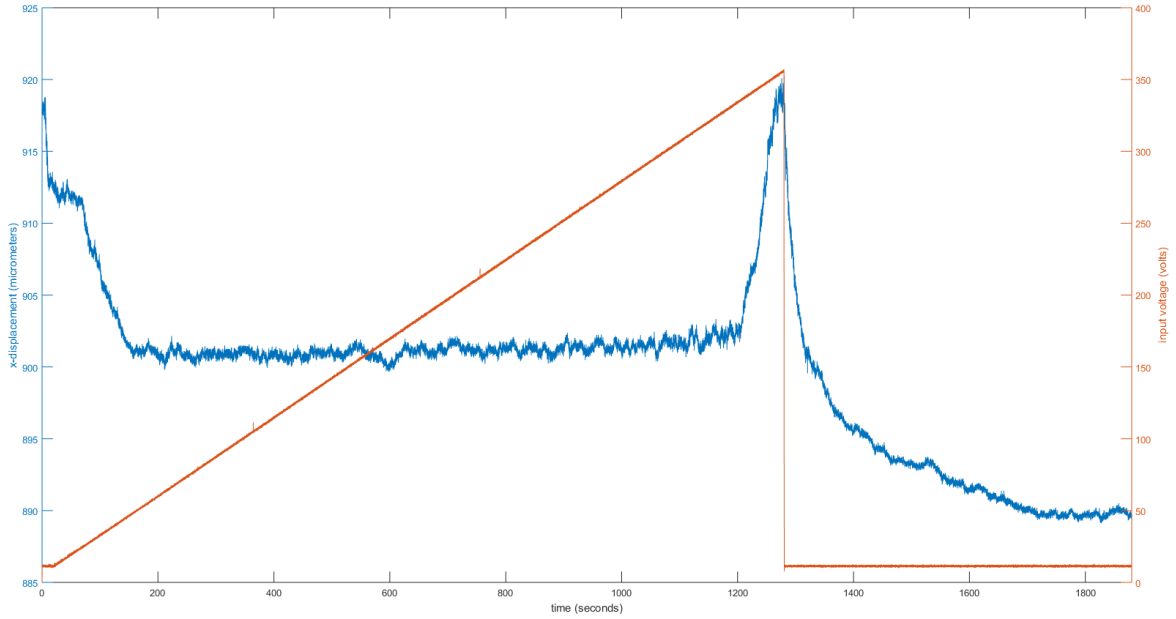

Figure C.18: The x-axis strain response for a 50 V ramp input until 360 V for T=180 seconds

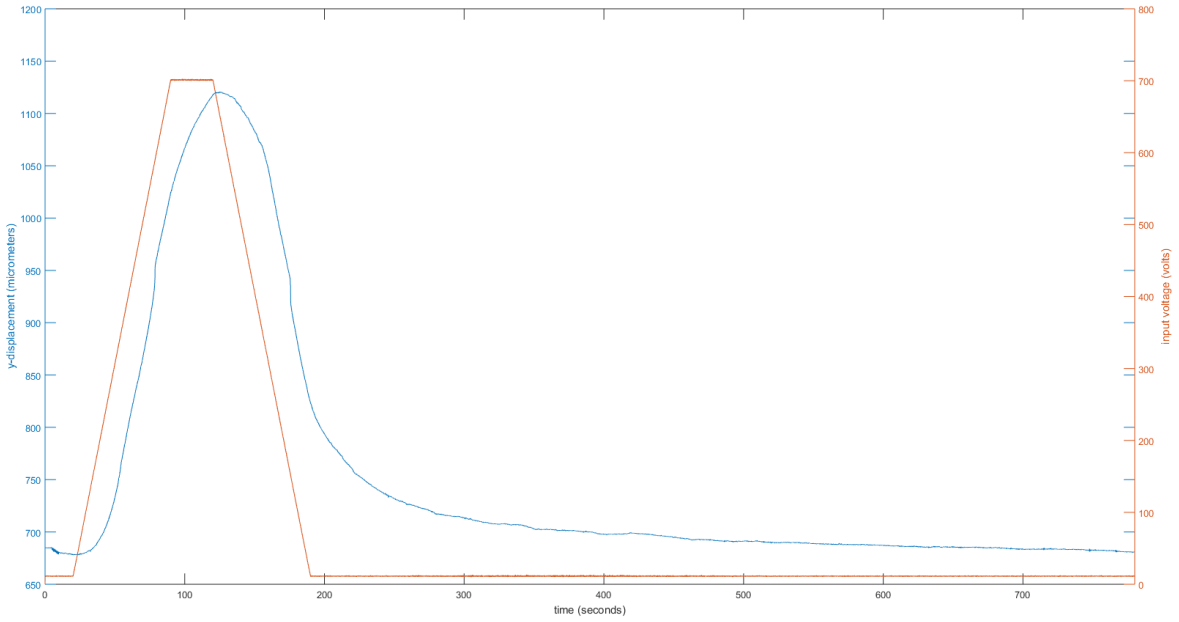

Figure C.19: The y-axis strain response for a 100 V symmetric ramp input until 700 V for T=10 seconds

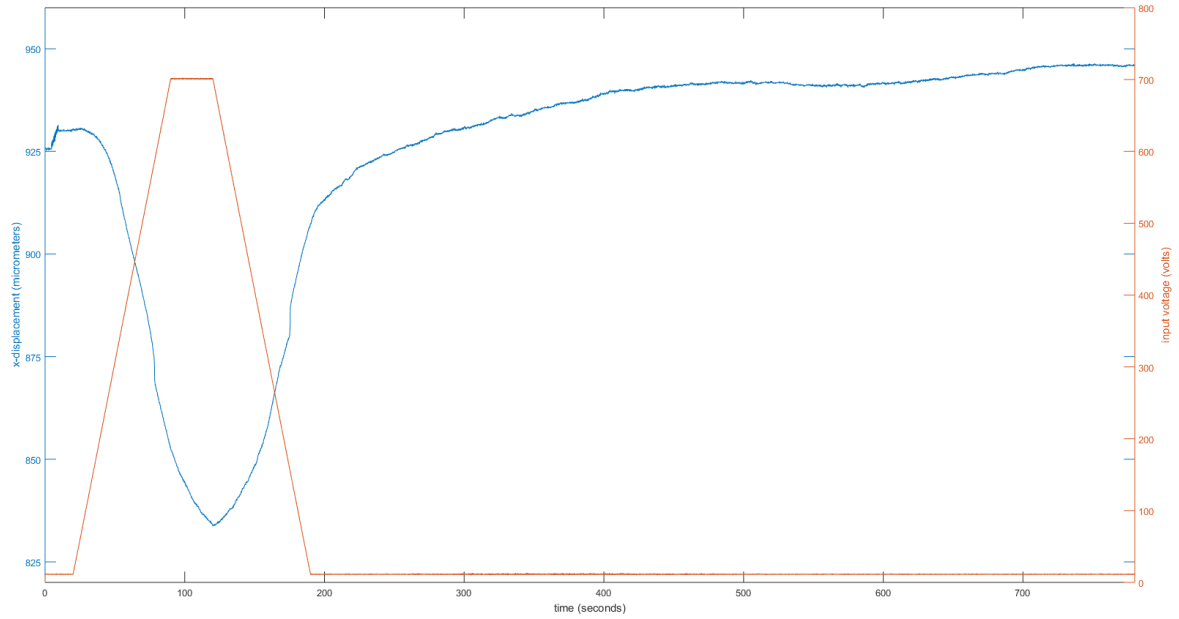

Figure C.20: The x-axis strain response for a 100 V symmetric ramp input until 700 V for T=10 seconds

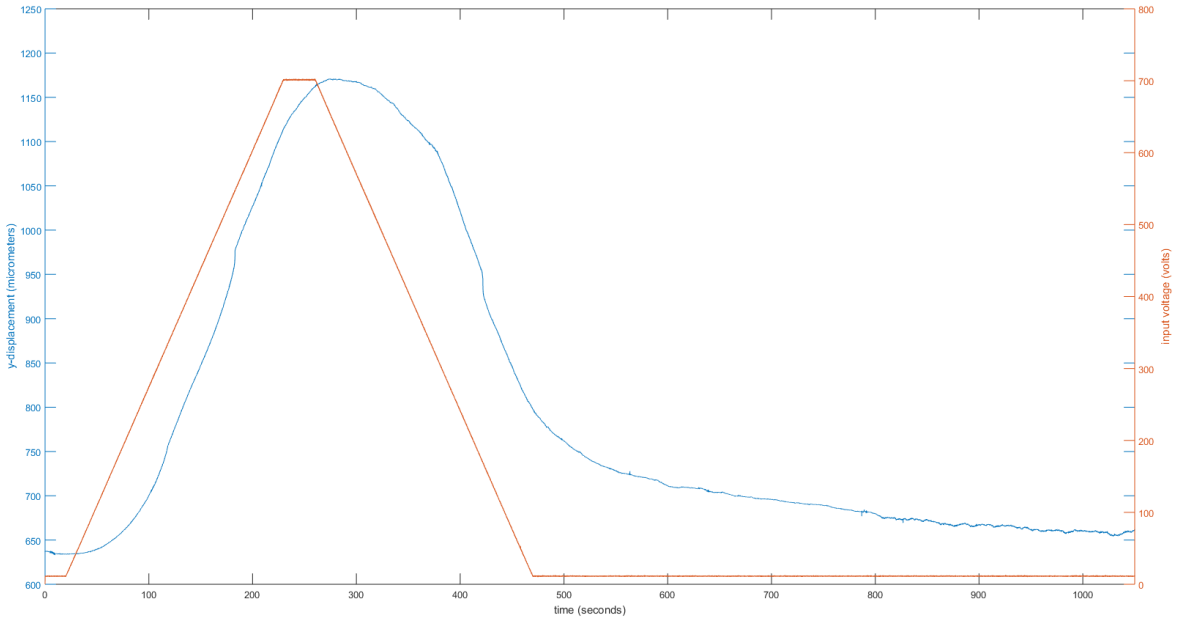

Figure C.21: The y-axis strain response for a 100 V symmetric ramp input until 700 V for T=30 seconds

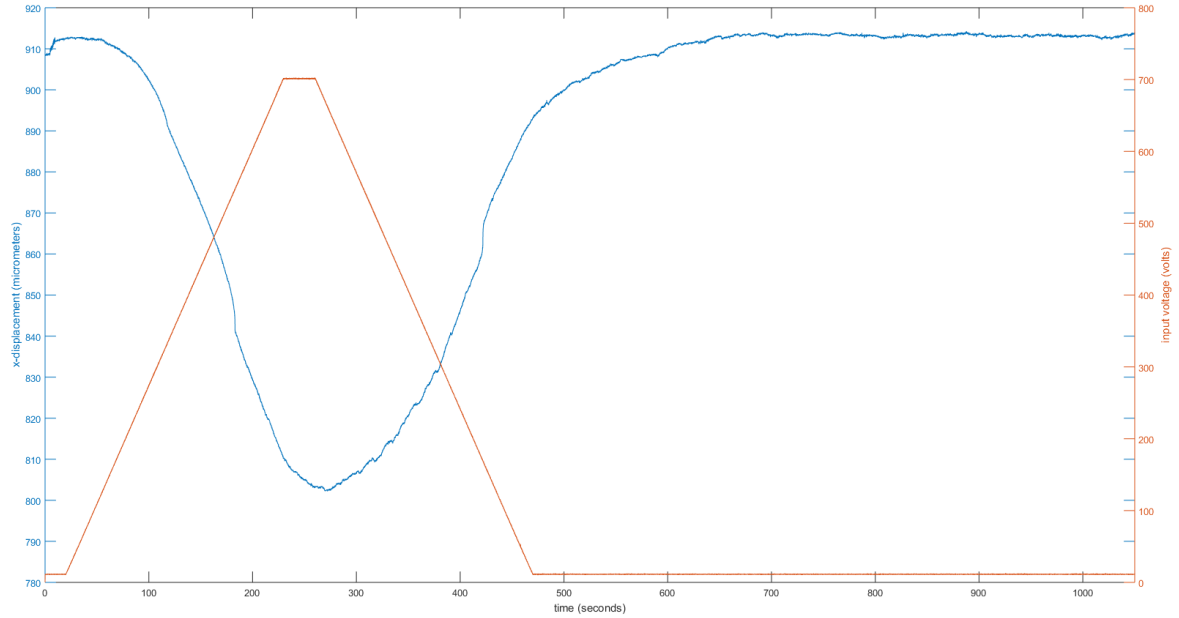

Figure C.22: The x-axis strain response for a 100 V symmetric ramp input until 700 V for T=30 seconds

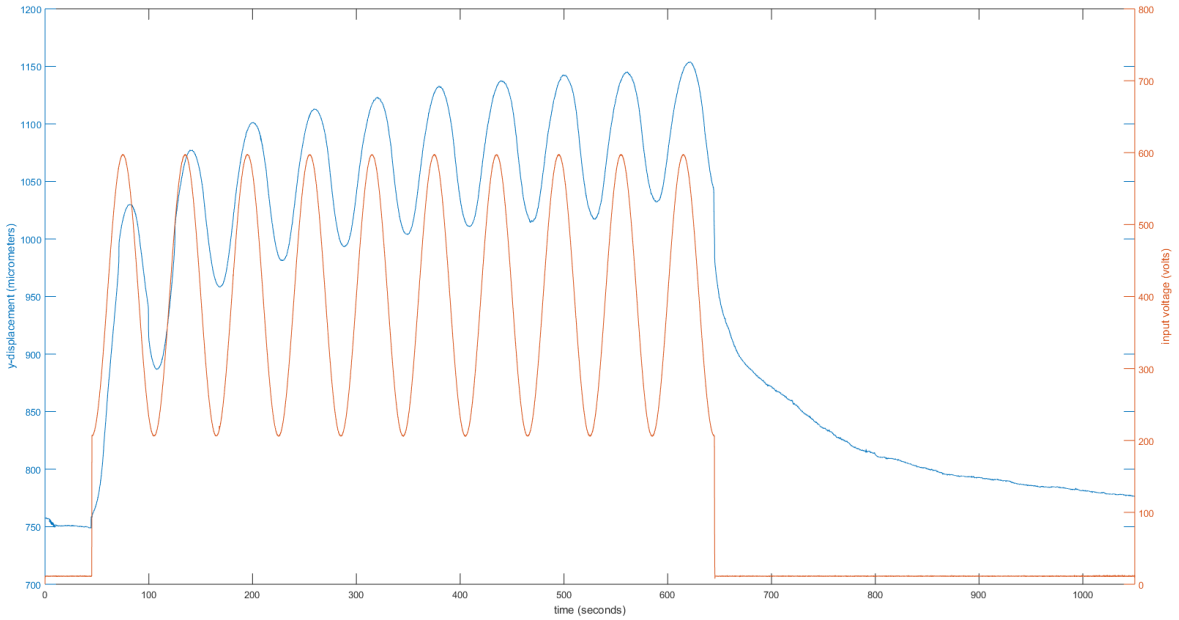

Figure C.23: The y-axis strain response for a sine wave with 200 V amplitude and 10 revolutions in 600 seconds

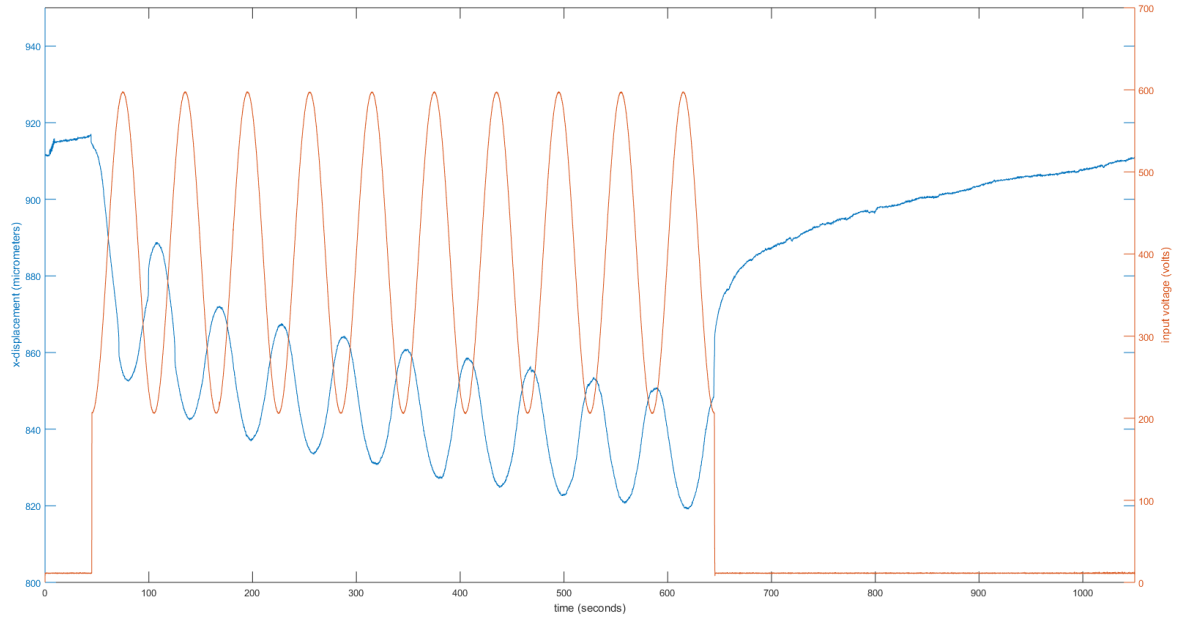

Figure C.24: The x-axis strain response for a sine wave with 200 V amplitude and 10 revolutions in 600 seconds

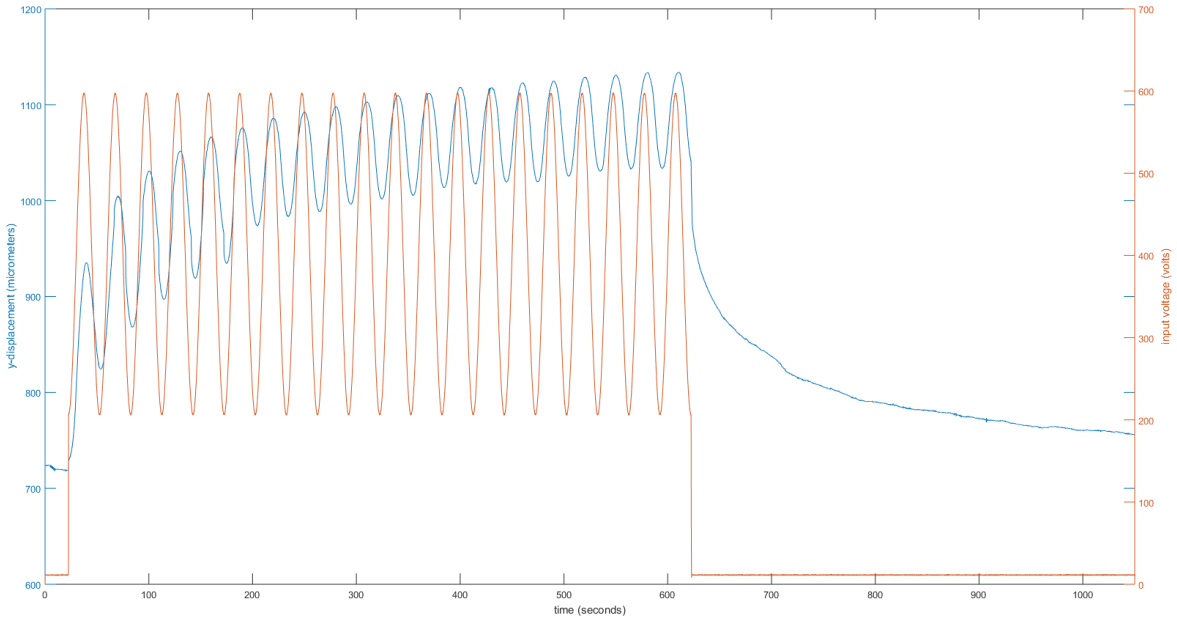

Figure C.25: The y-axis strain response for a sine wave with 200 V amplitude and 20 revolutions in 600 seconds

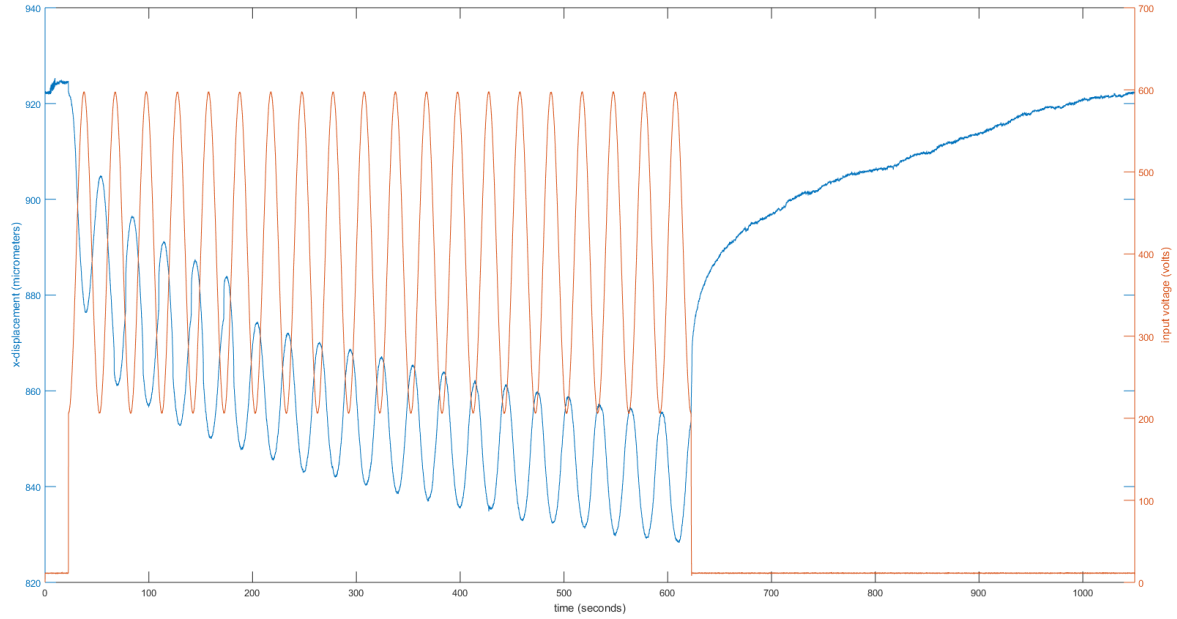

Figure C.26: The x-axis strain response for a sine wave with 200 V amplitude and 20 revolutions in 600 seconds

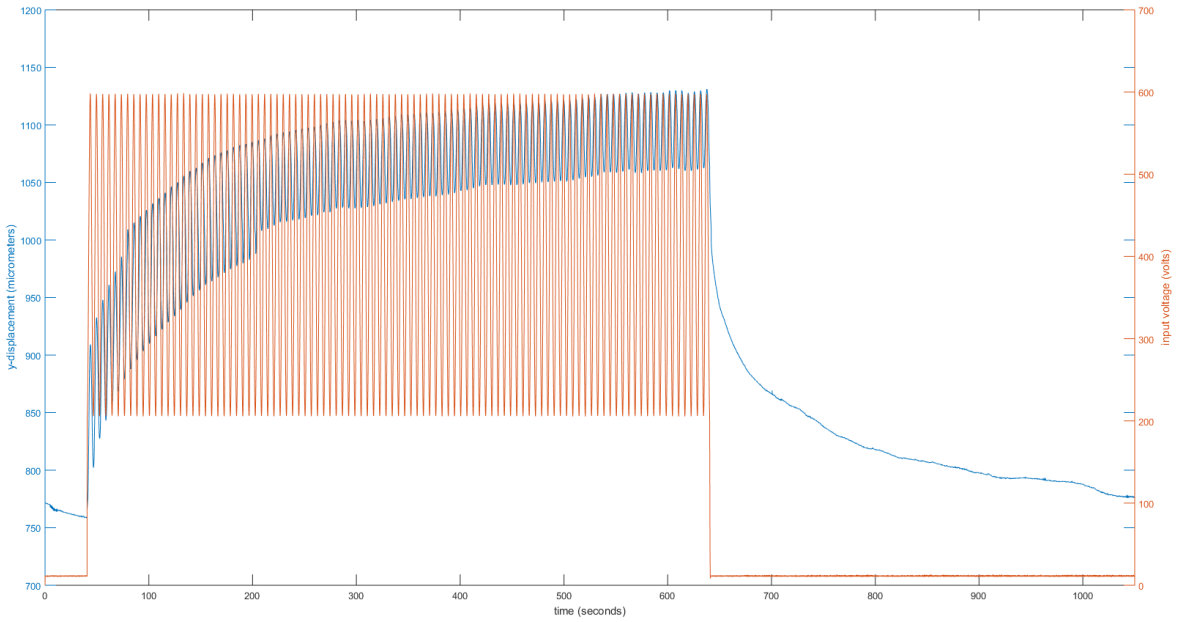

Figure C.27: The y-axis strain response for a sine wave with 200 V amplitude and 100 revolutions in 600 seconds

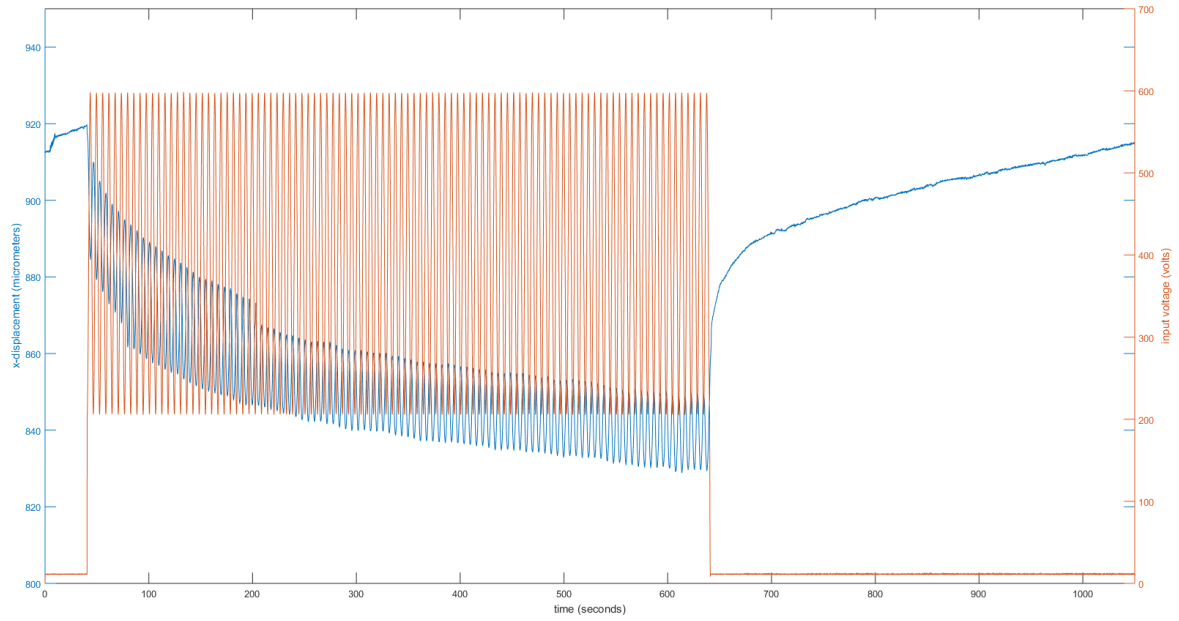

Figure C.28: The x-axis strain response for a sine wave with 200 V amplitude and 100 revolutions in 600 seconds

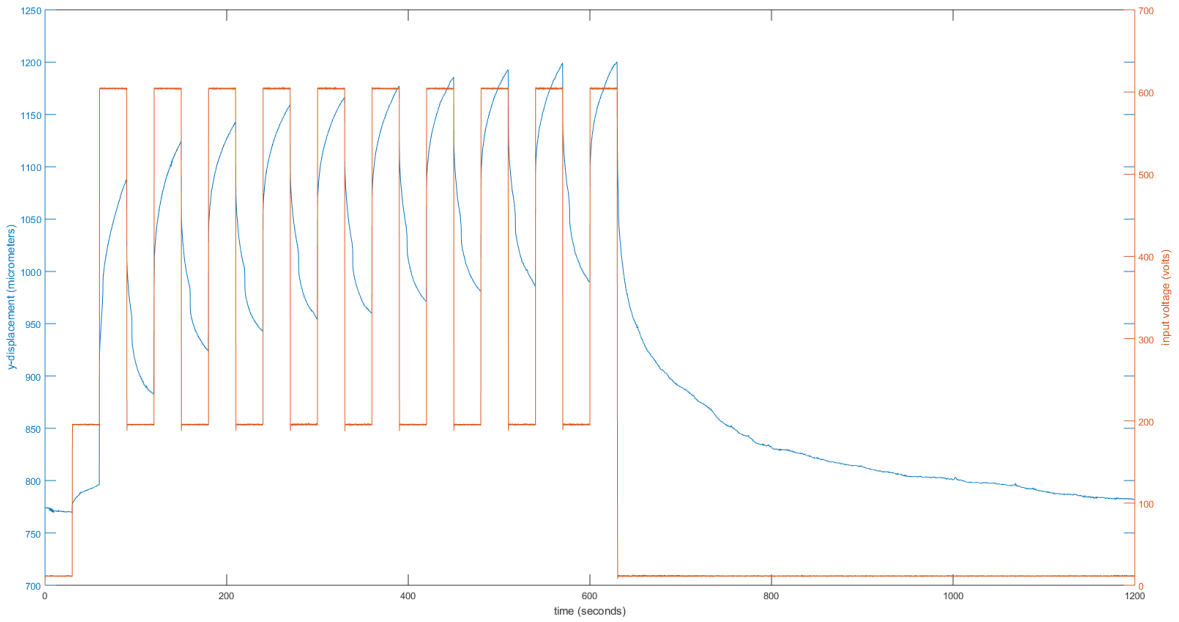

Figure C.29: The y-axis strain response for a square wave with 200 V amplitude and 10 revolutions in 600 seconds

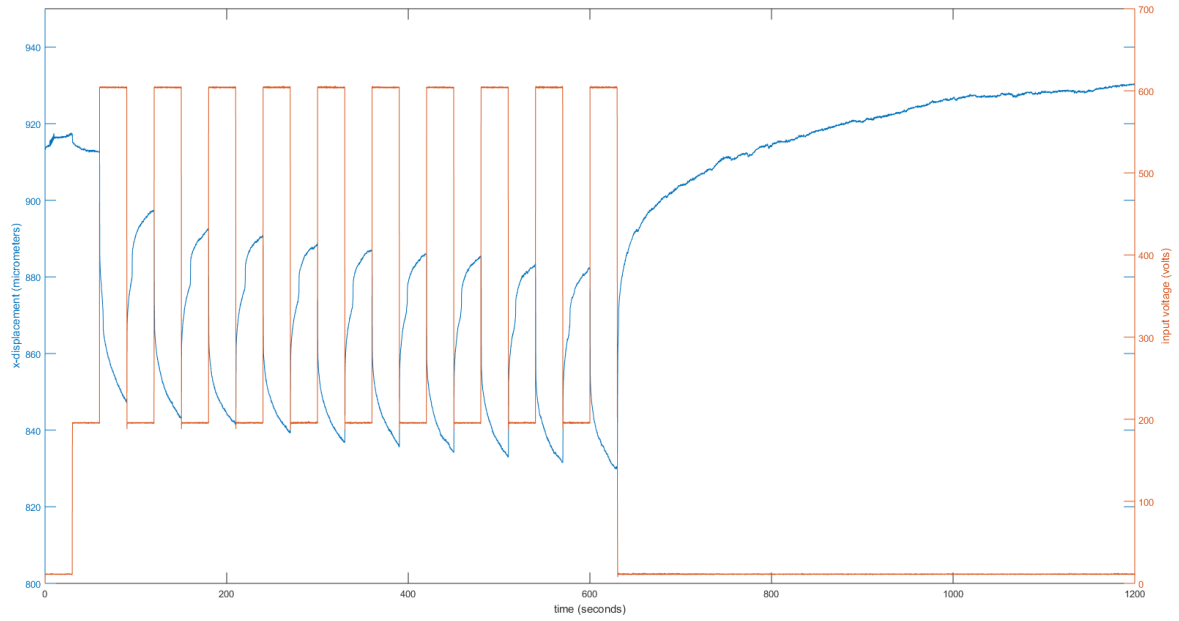

Figure C.30: The x-axis strain response for a square wave with 200 V amplitude and 10 revolutions in 600 seconds

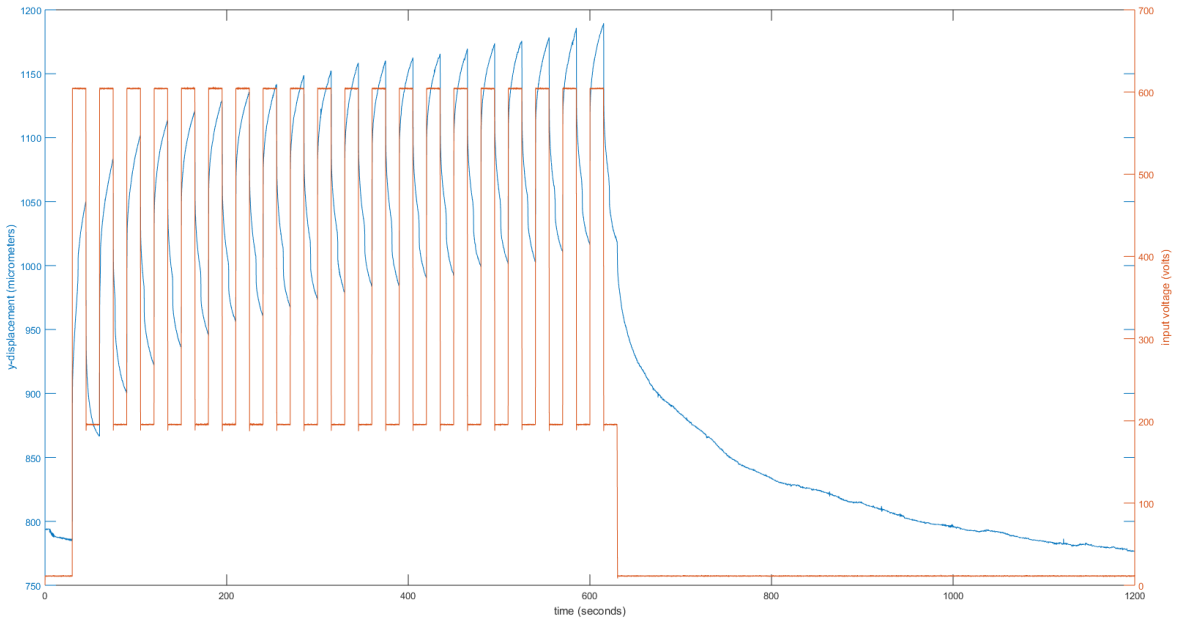

Figure C.31: The y-axis strain response for a square wave with 200 V amplitude and 20 revolutions in 600 seconds

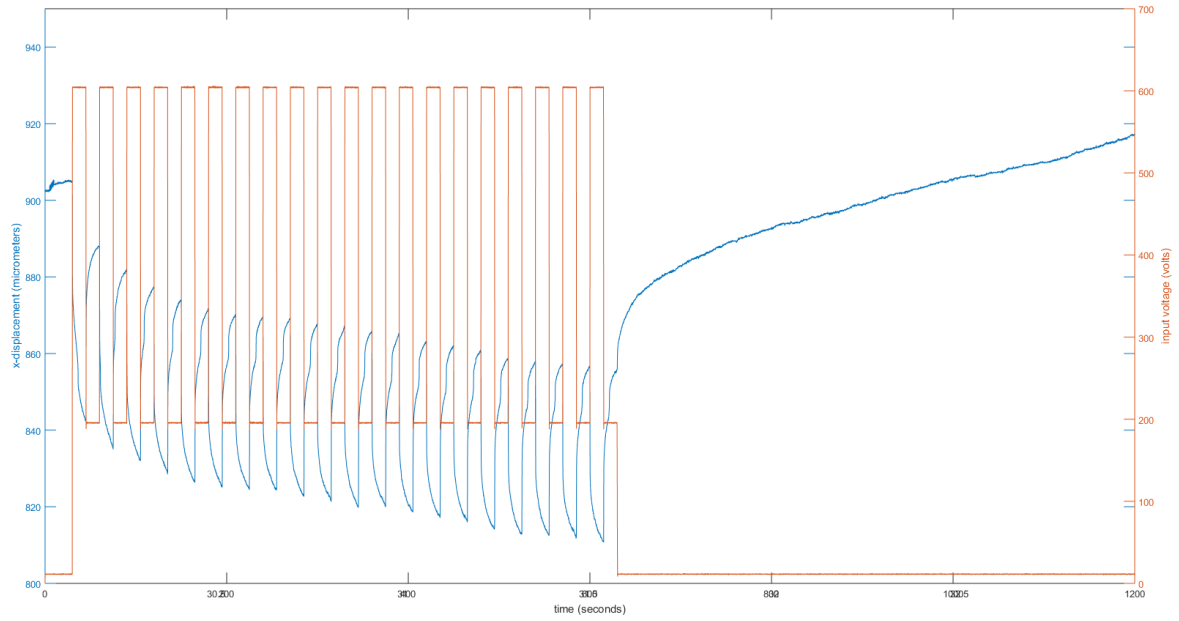

Figure C.32: The x-axis strain response for a square wave with 200 V amplitude and 20 revolutions in 600 seconds

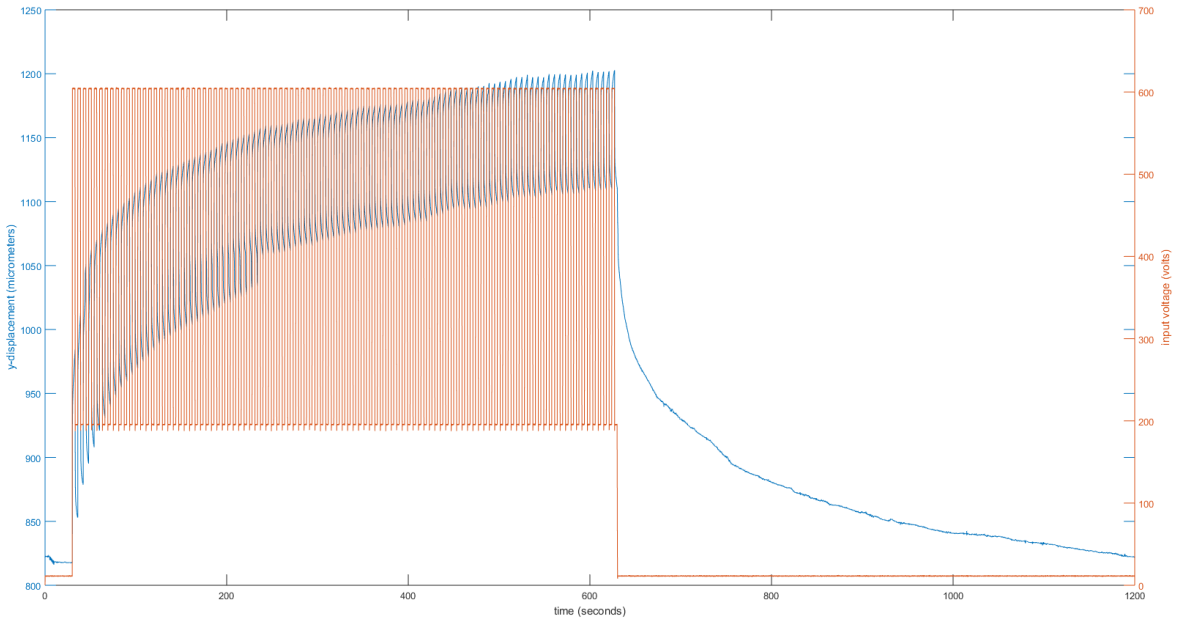

Figure C.33: The y-axis strain response for a square wave with 200 V amplitude and 100 revolutions in 600 seconds

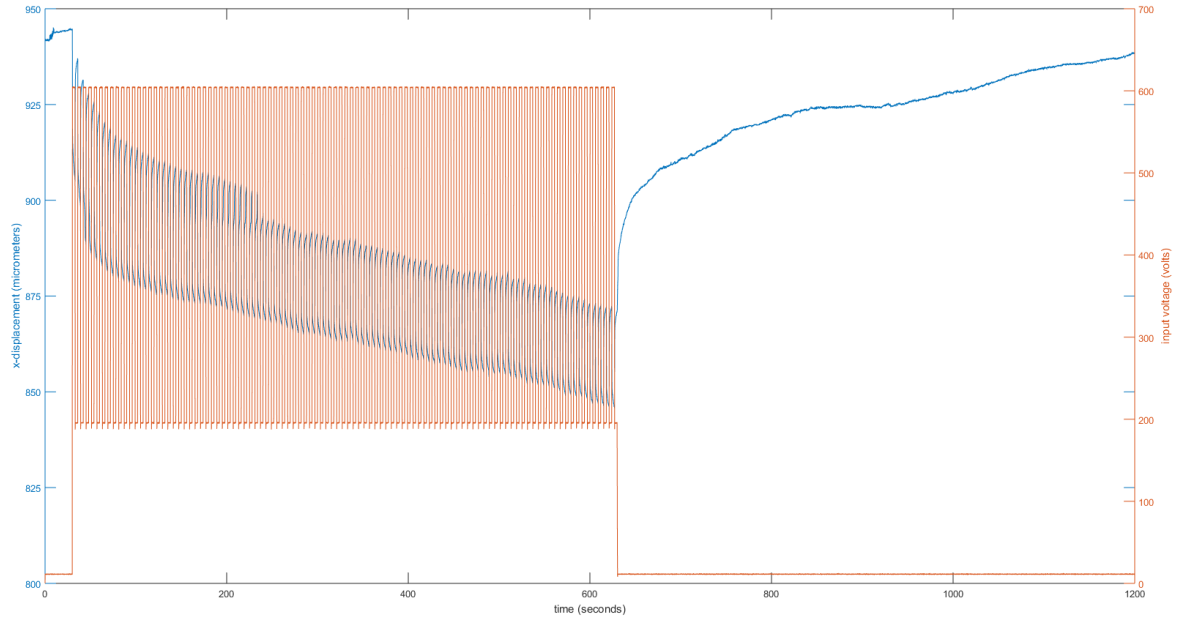

Figure C.34: The x-axis strain response for a square wave with 200 V amplitude and 100 revolutions in 600 seconds

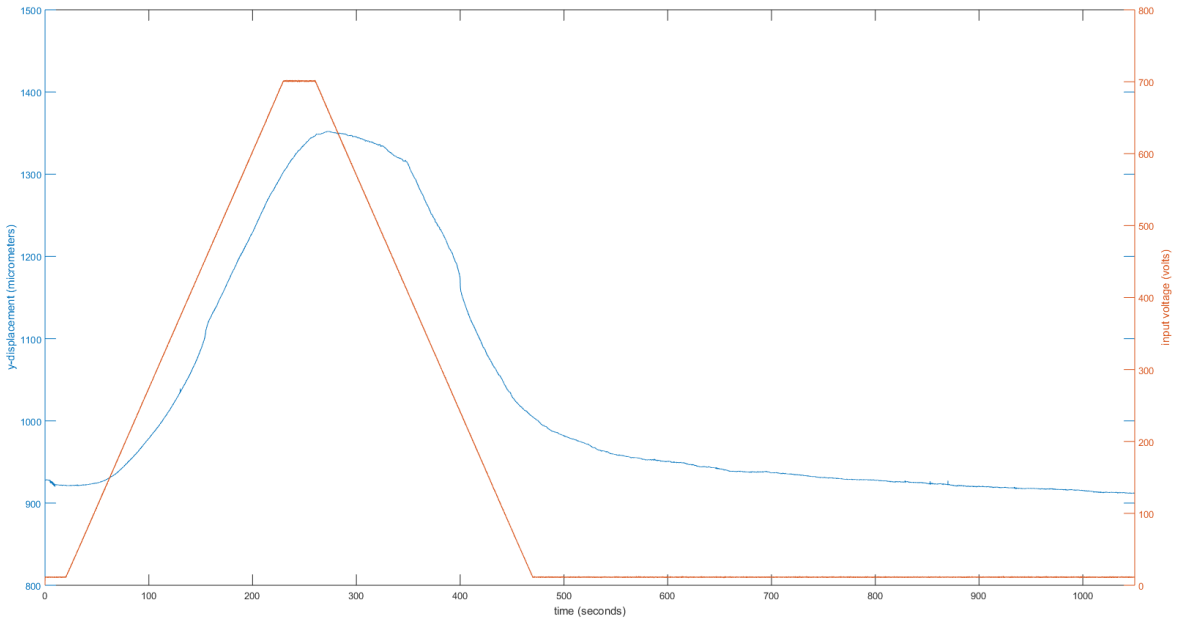

Figure C.35: The y-axis strain response for a 100 V symmetric ramp input until 700 V for T=30 seconds with reversed polarity

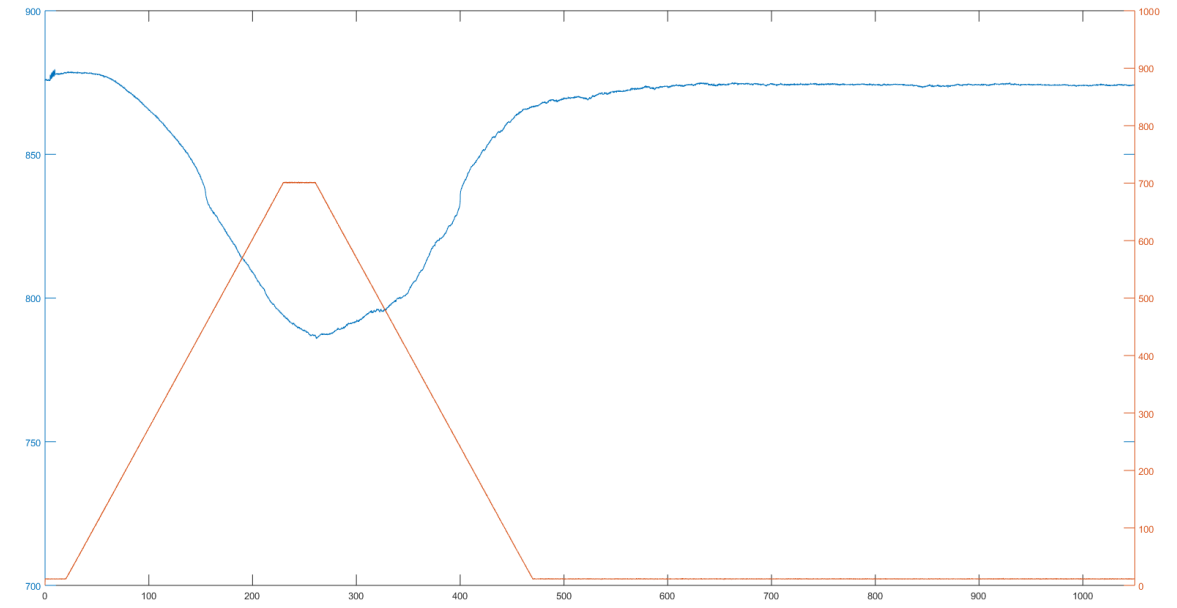

Figure C.36: The x-axis strain response for a 100 V symmetric ramp input until 700 V for T=30 seconds with reversed polarity

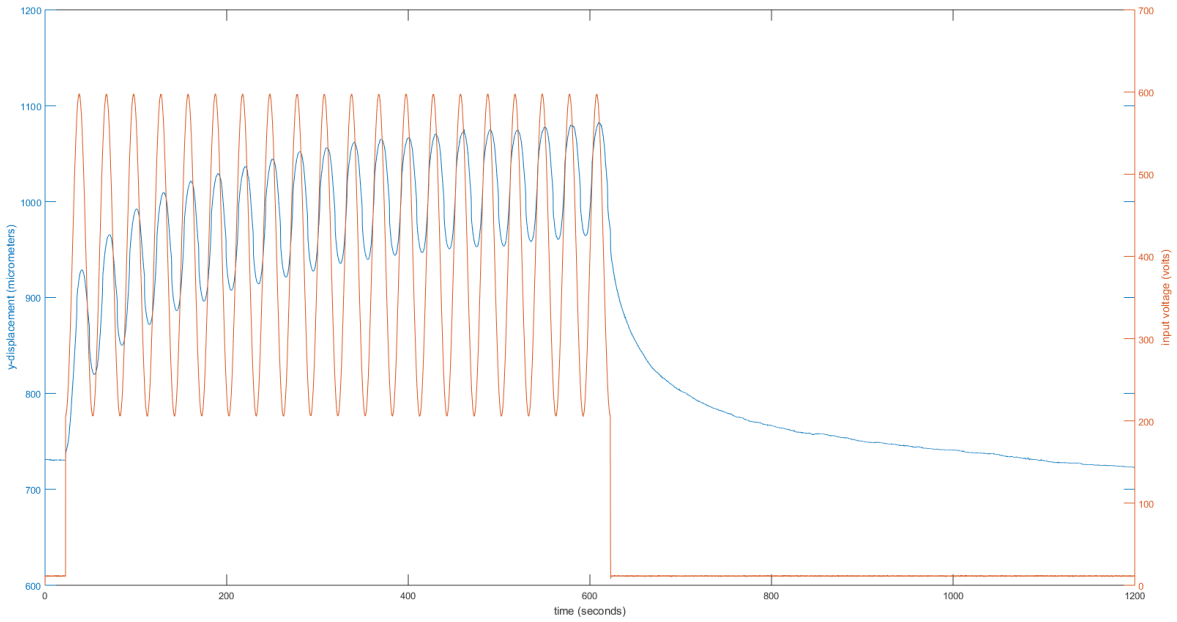

Figure C.37: The y-axis strain response for a sine wave with 200 V amplitude and 20 revolutions in 600 seconds with reversed polarity

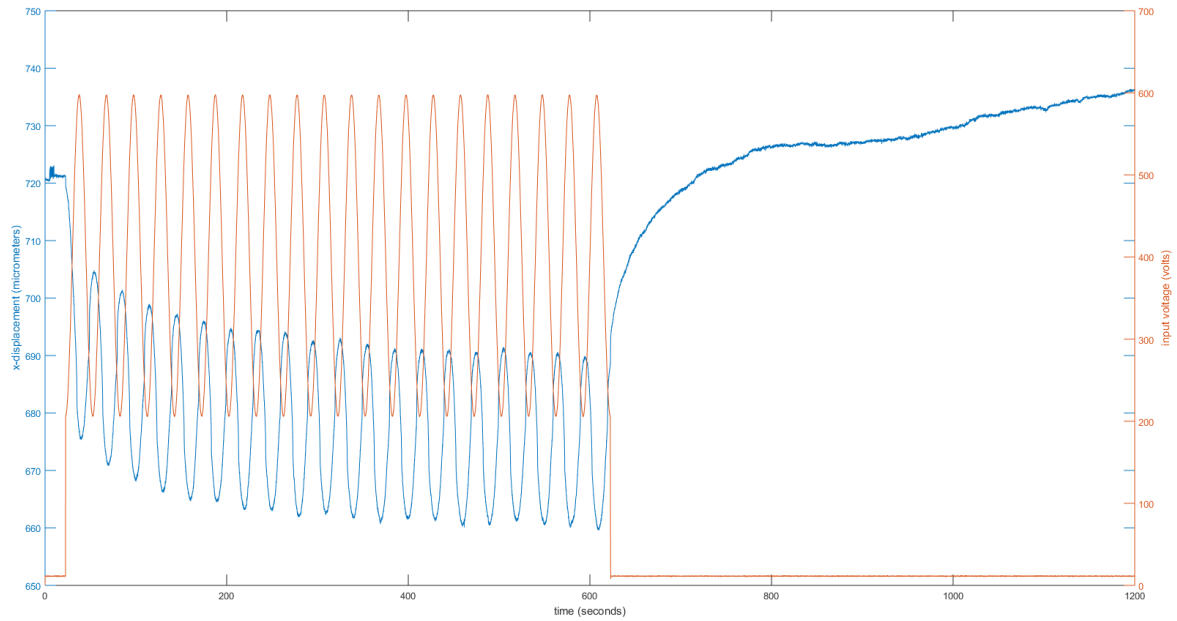

Figure C.38: The x-axis strain response for a sine wave with 200 V amplitude and 20 revolutions in 600 seconds with reversed polarity